

THE GAUSSIAN WAVE PACKET TRANSFORM VIA QUADRATURE RULES

PAUL BERGOLD AND CAROLINE LASSER

ABSTRACT. We study variants of the Gaussian wave packet transform and investigate their connection to the FBI transform. Based on the Fourier inversion formula and a partition of unity, which is formed by a collection of Gaussian basis functions, a new representation of square integrable functions is presented. Including a rigorous error analysis, the variants of the wave packet transform are then derived by a discretization of the Fourier integral via different quadrature rules. Based on Gauss–Hermite quadrature, we introduce a new representation of Gaussian wave packets in which the number of basis functions is significantly reduced. Numerical experiments in 1D illustrate the theoretical results.

1. INTRODUCTION

Gaussian functions and their generalizations occur in almost all fields of study. From simulations of quantum dynamics based on Gaussian wave packets to filter design in signal processing: Gaussian functions have been proven to have outstanding properties and are used in many models today. In the present paper, we focus on a question that is motivated by the development of numerical methods for quantum molecular dynamics and concerns the representation of wave functions:

How can a given wave function be efficiently decomposed into
a linear combination of Gaussian wave packets?

Using a slightly different wording, this question can be found in numerous fields. For example in numerical analysis, where Gaussians are used in the form of radial basis function (RBF) interpolations to construct solutions to PDEs, see [LF03], in widely used applications of statistics, in which probability densities are approximated by Gaussian mixtures, see [TSM85], or in seismology, where Gaussians appear in connection with the Gabor transform and are used for the decomposition of seismic waves, see [ML01]. With an eye on quantum dynamics, Gaussian superpositions appear in many state-of-the-art techniques to approximate solutions to the Schrödinger equation, such as the variational multi-configuration Gaussian wave packet (vMCG) method, see [WRB04], which is derived from the multi-configuration time-dependent Hartree (MCTDH) method, see [MMC90], and uses time-dependent (frozen) Gaussian functions as a basis set. In particular, the same wave function ansatz is used for the spawning method, see [MBNL96], and its direct dynamics implementation, known as ab initio multiple spawning, see [BNM00].

Recently, Batista et al. have proposed the time-sliced thawed Gaussian (TSTG) method for the propagation of Gaussian wave packets, see [KMB16]. A closer look at this method shows, that in the first step a given Gaussian wave packet is decomposed into a linear combination of Gaussian basis functions. In this way, the

Date: October 8, 2020.

2010 Mathematics Subject Classification. 42A38, 65D32, 65Z05, 81Q20.

Key words and phrases. Gaussian wave packet transforms, FBI transform, Quadrature rules, Schrödinger equation.

computation of the time-evolution is transferred to the propagation of each basis function. This initialization step is performed according to the fast Gaussian wave packet transform approach, which was introduced by Qian and Ying in [QY10]. While Batista et al. use plain Gaussians, Qian and Ying work with compactly supported basis functions that approximate a Gaussian profile and construct a representation for arbitrary L^2 -functions. The wave packet transform of Qian and Ying and thus also the initialization used by Batista et al. show a close connection to the FBI transform, which can be understood as a short time Fourier transform (STFT), or more precisely, a Gabor transform, see [FS98, Gab46]. In microlocal analysis, the FBI transform is used to analyze the distribution of a wave packet in position and momentum space simultaneously, see e.g. [Mar02]. Similar to the Fourier transform, there exists an inversion formula, see e.g. [LL20, Proposition 5.1], which yields that any function $\psi \in L^2(\mathbb{R}^d)$ can be decomposed as

$$(1.1) \quad \psi = (2\pi\varepsilon)^{-d} \int_{\mathbb{R}^{2d}} \langle g_z, \psi \rangle g_z \, dz,$$

where $\varepsilon > 0$ is a small parameter and the semiclassically scaled wave packet g_z with phase space center $z = (q, p) \in \mathbb{R}^{2d}$ is defined for a given Schwartz function $g: \mathbb{R}^d \rightarrow \mathbb{C}$ of unit norm, that could be but needn't be a Gaussian, by

$$(1.2) \quad g_z(x) := g(x - q) e^{ip \cdot (x - q)/\varepsilon}, \quad x \in \mathbb{R}^d.$$

We note that there are different conventions in the literature for the phase factor of the wave packet g_z . For example, in [CR12] the authors work with $e^{ip \cdot (x - q)/\varepsilon}$, which results from the action of the Weyl-Heisenberg translation operator. Also the wave packet amplitude is often scaled according to $\varepsilon^{-d/4} g((x - q)/\sqrt{\varepsilon})$.

The representation of Qian and Ying can be viewed as a discrete version of (1.1). In order to arrive at their representation, the phase space integral is discretized via Riemann sums on uniform Cartesian grids. We would like to point out that the discrete FBI inversion is closely related to Gabor frames and Gabor expansions and refer to [Grö01] for a broader perspective. Moreover, we note that the original FBI inversion in (1.1) can be used to construct solutions to the semiclassical Schrödinger equation, based on either thawed or frozen evolving Gaussians, see e.g. [LL20], as well as for the initialization of Gaussian beams, see [LQ09, Zhe14].

In the present paper, we propose a different discretization of the phase space integral, which significantly reduces the number of basis functions compared to Riemann sums. Therefore, we introduce a new representation of L^2 -functions that consists of a discrete and a continuous component and can be viewed as a preliminary stage of the discrete FBI inversion. The discrete part is based on a summation curve and a partition of unity, which are both formed by the underlying Gaussian basis functions. In particular, it was assumed by Batista et al. that the basis functions are closely overlapping and uniformly distributed in order to ensure that the summation curve can be approximated by a constant value. Our new representation relies on a more general definition of this summation curve. The continuous part is based on the Fourier inversion formula, which is used to represent the cutouts of the original wave packet produced by the action of the partition. By discretizing the Fourier integral via different quadrature rules, we then obtain approximations of a Gaussian wave packet $\Psi: \mathbb{R}^d \rightarrow \mathbb{C}$ of the form

$$\Psi(x) \approx \frac{1}{S(\Gamma_q; x)} \sum_{k \in \Gamma_q} \sum_{j \in \Gamma_p^{(\text{rule})}} r_{j,k}^{(\text{rule})} g_{j,k}(x),$$

where the basis functions $g_{j,k}$ correspond to the wave packet g_z in (1.2) for a Gaussian amplitude g centered in grid points $(q_k, p_j) \in \mathbb{R}^{2d}$, $S(\Gamma_q; \bullet)$ denotes the

summation curve associated with the position grid $\{q_k\}_{k \in \Gamma_q}$, and the representation coefficients $r_{j,k}^{(\text{rule})}$ are complex numbers, depending on the quadrature rule. Note that also the momentum grid depends on the chosen quadrature rule. We recognize the relation to the FBI inversion formula in (1.1) and mention that this seems to be the first time that a wave packet transform has been derived this way. In particular, our analysis establishes the connection between the results of Batista et al. (Gaussian basis functions), Qian and Ying (compactly supported basis functions that approximate a Gaussian profile) and the standard FBI transform. We note that Qian and Ying use the fast Fourier transform (FFT) to compute the representation coefficients, see [QY10, Algorithm 3.3], while our approach here enables fast computation by reducing the number of quadrature nodes.

Our main new result is a representation that is based on a discretization via Gauss–Hermite quadrature. This representation can be used to obtain excellent approximations of Gaussian wave packets with a significantly smaller number of grid points p_j in momentum space, that would be necessary for uniform grids. Using sparse-grid Gauss–Hermite quadrature, this representation can potentially be used in higher dimensions.

1.1. Outline. In §2 we study a new representation of a square integrable function $\psi \in L^2(\mathbb{R}^d)$, based on a decomposition of ψ into a sum of “Gaussian slices” and a representation via the Fourier inversion formula, see Proposition 2.4. Moreover, we discuss the connection to the inverse FBI transform and extend our result to the special case, where ψ is a Gaussian wave packet, see Lemma 2.6. Afterwards, in §3 we discuss the discretization via different quadrature rules. As a special candidate we consider Gauss–Hermite quadrature. The main new result of this paper can be found in Theorem 3.2, where we compare different variants of the Gaussian wave packet transform. Finally, we present numerical experiments in §4, that underline our theoretical results and illustrate the benefits of approximations based on Gauss–Hermite quadrature.

2. A WAVE PACKET REPRESENTATION INSPIRED BY THE FBI TRANSFORM

Let $d \geq 1$ and recall the definition of the semiclassically scaled wave packet g_z in (1.2). For a real symmetric and positive definite matrix $G \in \mathbb{R}^{d \times d}$ we consider the Gaussian function

$$(2.1) \quad g(x) := (\pi\varepsilon)^{-d/4} \det(G)^{1/4} \exp\left(-\frac{1}{2\varepsilon} x^T G x\right) \quad \text{for all } x \in \mathbb{R}^d.$$

We note that the dependency on G and ε is always assumed implicitly, and that in the one-dimensional setting we write γ instead of G . From now on, whenever we use the wave packet g_z in (1.2), we assume that g is a Gaussian defined according to (2.1).

2.1. Summation Curve. For a non-empty index set $\Gamma_q \subseteq \mathbb{Z}^d$ and grid points $\{q_k\}_{k \in \Gamma_q}$, we use shifted Gaussians to define the summation curve

$$(2.2) \quad S(\Gamma_q; x) := \sum_{k \in \Gamma_q} g(x - q_k)^2, \quad x \in \mathbb{R}^d.$$

In this paper, we always assume that the underlying grid points q_k are uniformly distributed, although nonuniform distributions are also possible. The convergence of the series for uniform grids is guaranteed by the next lemma. Let us focus on the one-dimensional setting for a moment. A quick look at Figure 1 makes it plausible, that for $\Gamma_q = \mathbb{Z}$ and a sufficiently small uniform grid spacing $\Delta q > 0$ the summation curve can be approximated by a constant value. The lemma tells us, that this constant equals $1/\Delta q$:

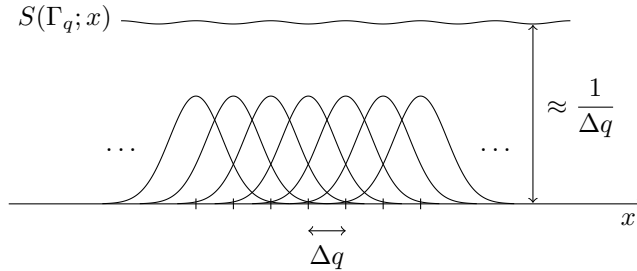


FIGURE 1. Squared Gaussians $g(\bullet - q_k)^2$ and the summation curve $S(\Gamma_q; \bullet)$ on a uniform grid for $d = 1$. By Lemma 2.1, the summation curve can be approximated by the constant value $1/\Delta q$.

Lemma 2.1. *Consider the Gaussian function in (2.1) for $d = 1$ and a positive width parameter $\gamma > 0$. Then, for $\Gamma_q = \mathbb{Z}$ and uniform grid points $q_k = k\Delta q$ with distance $\Delta q > 0$, the summation curve $S(\Gamma_q; x)$ has the expansion*

$$(2.3) \quad S(\Gamma_q; x) = \frac{1}{\Delta q} + \frac{2}{\Delta q} \sum_{n=1}^{\infty} \cos\left(\frac{2\pi n x}{\Delta q}\right) \exp\left(-\frac{\pi^2 n^2 \varepsilon}{\gamma(\Delta q)^2}\right),$$

where the convergence is uniform in $x \in \mathbb{R}$. In particular, we obtain spectral convergence of the summation curve to $1/\Delta q$ as $\Delta q \rightarrow 0$, that is, for all $s \in \mathbb{N}$, there exists a positive constant $c_s > 0$, depending on s, ε and γ , such that

$$\left| S(\Gamma_q; x) - \frac{1}{\Delta q} \right| \leq c_s \cdot (\Delta q)^{2s-1} \quad \text{for all } x \in \mathbb{R},$$

where the constant can be chosen as

$$c_s = \frac{2s! \gamma^s}{\pi^{2s} \varepsilon^s}.$$

Moreover, the summation curve is Δq -periodic and infinitely differentiable.

We present the proof in Appendix A. Moreover, we show that the expansion in (2.3) can also be used in higher dimensions, provided that the grid $\{q_k\}_{k \in \Gamma_q}$ is aligned to the eigenvectors of the width matrix $G \in \mathbb{R}^{d \times d}$.

The definition of the summation curve $S(\Gamma_q; \bullet) > 0$ in (2.2) allows to construct the functions $\chi_k(x) := g(x - q_k)^2 / S(\Gamma_q; x)$, which satisfy the two conditions

$$(2.4) \quad 0 < \chi_k(x) \leq 1 \quad \text{and} \quad \sum_{k \in \Gamma_q} \chi_k(x) = 1 \quad \text{for all } x \in \mathbb{R}^d.$$

Hence, the family $\{\chi_k\}_{k \in \Gamma_q}$ builds a so-called partition of unity. Partitions of unity typically occur in the theory of manifolds, see e.g. [Tu11, §13.1], but are also used in the numerical community, e.g. to solve differential equations, see [GS00, §4.1.2].

In the next step we combine the partition $\{\chi_k\}_{k \in \Gamma_q}$ with the Fourier inversion formula to obtain a decomposition of square integrable functions.

2.2. A Representation via the Inverse Fourier Transform. In some situations it is useful to analyze the distribution of a wave packet in position and momentum space simultaneously. A central tool for this microlocalization is provided by the *Fourier-Bros-Iagolnitzer* (in short: FBI) transform:

Definition 2.2. For a point $z = (q, p) \in \mathbb{R}^{2d}$ in phase space, consider the Gaussian wave packet g_z . Then, the mapping

$$T^\varepsilon: \mathcal{S}(\mathbb{R}^d) \rightarrow \mathcal{S}(\mathbb{R}^{2d}), \quad (T^\varepsilon \psi)(z) := (2\pi\varepsilon)^{-d} \langle g_z, \psi \rangle,$$

is called the FBI transform.

Remark 2.3. We denote by $\mathcal{S}(\mathbb{R}^d)$ the Schwartz class in \mathbb{R}^d . Moreover, the inner product $\langle \bullet, \bullet \rangle$ in $L^2(\mathbb{R}^d)$ is taken antilinear in its first and linear in its second argument.

The FBI transform can be extended to an isometry from $L^2(\mathbb{R}^d)$ to $L^2(\mathbb{R}^{2d})$ and it is proven in [Mar02, chapter 3.1], that the inversion formula in (1.1) holds for all functions $\psi \in L^2(\mathbb{R}^d)$. This formula can be used for approximation schemes to the time-dependent semiclassical Schrödinger equation. The major types of such approximations are based on either thawed or frozen evolving Gaussians, corresponding to Gaussian beams or the Herman-Kluk propagator, see [LL20, §5].

We work with the ε -rescaled Fourier transform $\mathcal{F}_\varepsilon: L^2(\mathbb{R}^d) \rightarrow L^2(\mathbb{R}^d)$,

$$\mathcal{F}_\varepsilon \psi(p) := (2\pi\varepsilon)^{-d/2} \int_{\mathbb{R}^d} \psi(x) e^{-ip \cdot x / \varepsilon} dx \quad \text{for all } p \in \mathbb{R}^d.$$

Using its inversion formula, we obtain a new representation that is connected to the inversion formula (1.1) of the FBI transform.

Proposition 2.4 (Representation via inverse FT).

Let $\psi \in \mathcal{S}(\mathbb{R}^d)$. For a point $z = (q, p) \in \mathbb{R}^{2d}$ recall the definition of g_z in (1.2) and introduce the map

$$(2.5) \quad x \mapsto \mathcal{I}_q(x) := (2\pi\varepsilon)^{-d} \int_{\mathbb{R}^d} \langle g_z, \psi \rangle g_z(x) dp.$$

Moreover, let $\{q_k\}_{k \in \Gamma_q}$ be an arbitrary grid in the position space. Then, for all $x \in \mathbb{R}^d$, we have

$$(2.6) \quad \psi(x) = \frac{1}{S(\Gamma_q; x)} \sum_{k \in \Gamma_q} \mathcal{I}_{q_k}(x) \quad \text{and}$$

$$(2.7) \quad \psi(x) = \int_{\mathbb{R}^d} \mathcal{I}_q(x) dq.$$

For convenience of the proof we take $\psi \in \mathcal{S}(\mathbb{R}^d)$, but we note that the above representations extend directly to $L^2(\mathbb{R}^d)$.

Proof. Let $\psi \in \mathcal{S}(\mathbb{R}^d)$. We start to prove the upper representation. We denote $g_k(x) := g(x - q_k)$, where the Gaussian amplitude g is defined in (2.1). According to the properties of the partition of unity $\{\chi_k\}_{k \in \Gamma_q}$ in (2.4), the function ψ can be decomposed into a sum of Gaussian slices as follows:

$$(2.8) \quad \psi = \psi \sum_{k \in \Gamma_q} \chi_k = \psi \left(\frac{1}{S(\Gamma_q; \bullet)} \sum_{k \in \Gamma_q} g_k^2 \right) = \frac{1}{S(\Gamma_q; \bullet)} \sum_{k \in \Gamma_q} (\psi g_k) g_k.$$

In particular, since $g_k \in \mathcal{S}(\mathbb{R}^d)$ for all $k \in \Gamma_q$, we conclude that $\psi g_k \in \mathcal{S}(\mathbb{R}^d)$ and therefore, using the Fourier inversion theorem, we obtain for all $x \in \mathbb{R}^d$:

$$(2.9) \quad (\psi g_k)(x) = (2\pi\varepsilon)^{-d/2} \int_{\mathbb{R}^d} \mathcal{F}_\varepsilon[\psi g_k](p) e^{ix \cdot p / \varepsilon} dp,$$

where we have for all $p \in \mathbb{R}^d$:

(2.10)

$$\begin{aligned} \mathcal{F}_\varepsilon[\psi g_k](p) e^{ix \cdot p/\varepsilon} g_k(x) &= (2\pi\varepsilon)^{-d/2} \int_{\mathbb{R}^d} \psi(y) g_k(y) e^{-ip \cdot (y - q_k)/\varepsilon} dy g_k(x) e^{ip \cdot (x - q_k)/\varepsilon} \\ &= (2\pi\varepsilon)^{-d/2} \langle g_{(q_k, p)}, \psi \rangle g_{(q_k, p)}(x). \end{aligned}$$

Consequently, by inserting (2.9) and (2.10) into (2.8), we conclude that

$$\psi(x) = \frac{1}{S(\Gamma_q; x)} \sum_{k \in \Gamma_q} \mathcal{I}_{q_k}(x).$$

For the second representation in (2.7) we use that g is of unit norm, $\|g\|_{L^2(\mathbb{R}^d)} = 1$. Hence, for all $x \in \mathbb{R}^d$, we get

$$\psi(x) = \psi(x) \int_{\mathbb{R}^d} |g(x - q)|^2 dq = \int_{\mathbb{R}^d} (\psi(x) g(x - q)) g(x - q) dq.$$

Thus, again by the Fourier inversion formula, we obtain for all $x \in \mathbb{R}^d$:

$$\begin{aligned} \psi(x) &= \int_{\mathbb{R}^d} \left((2\pi\varepsilon)^{-d/2} \int_{\mathbb{R}^d} \mathcal{F}_\varepsilon[\psi g(\bullet - q)](p) e^{ix \cdot p/\varepsilon} dp \right) g(x - q) dq \\ &= \int_{\mathbb{R}^d} \left((2\pi\varepsilon)^{-d} \int_{\mathbb{R}^d} \langle g_z, \psi \rangle g_z(x) dp \right) dq = \int_{\mathbb{R}^d} \mathcal{I}_q(x) dq, \end{aligned}$$

which makes the proof complete. \square

We notice that the representation of ψ in (2.6) can be viewed as an inversion of the FBI transform on the position grid $\{q_k\}_{k \in \Gamma_q}$. This connection becomes particularly clear in the one-dimensional case: We start from (2.7) and approximate the integral over $\mathcal{I}_q(x)$ using an infinite Riemann sum on a uniform grid of size Δq , which yields the approximation

$$\psi(x) \approx \Delta q \sum_{k \in \mathbb{Z}} \mathcal{I}_{q_k}(x).$$

Hence, the fact that $\Delta q \approx 1/S(\Gamma_q; x)$ for a small grid spacing Δq according to Lemma 2.1 establishes the connection to the representation in (2.6).

We now focus on the case where ψ is a Gaussian wave packet and thus only Gaussian integrals need to be performed. We note that non-Gaussian functions are also possible and have been studied by other authors. In particular, in Appendix B we discuss the wave packet transform of Qian and Ying [QY10] in the context of windowed Fourier series, which makes it possible to determine the decay rates of the representation coefficients.

2.3. A Representation for Gaussian Wave Packets. If ψ itself is a Gaussian wave packet, we recognize that for all $q \in \mathbb{R}^d$ the function $\mathcal{I}_q(x)$ can be read as the Fourier transform of a Gaussian and hence is Gaussian, too. In this subsection, we calculate an explicit formula for $\mathcal{I}_q(x)$.

For a complex symmetric matrix $C \in \mathbb{C}^{d \times d}$ with positive definite imaginary part (the set of all matrices with this property is known as the Siegel half-space, see [Sie43]) and a point $(q, p) \in \mathbb{C}^{2d}$ in the complex-valued phase-space, we define

$$(2.11) \quad \varphi[q, p, C](x) := \exp \left(\frac{i}{\varepsilon} \left(\frac{1}{2} (x - q)^T C (x - q) + p^T (x - q) \right) \right).$$

We note that φ is not normalized. Moreover, let us introduce the following notation for a real symmetric and positive definite matrix $A \in \mathbb{R}^{d \times d}$ and $x, y \in \mathbb{R}^d$:

$$\langle x, y \rangle_A := x^T A y, \quad \|x\|_A := \sqrt{\langle x, x \rangle_A}.$$

We start to present a formula for the Fourier transform $\mathcal{F}_\varepsilon[\psi g(\bullet - q)]$:

Lemma 2.5 (Product of Gaussians). *For $z_0 = (q_0, p_0) \in \mathbb{R}^{2d}$ and $C_0 \in \mathbb{C}^{d \times d}$ in the Siegel half-space, consider the normalized Gaussian wave packet*

$$\Psi(x) := (\pi\varepsilon)^{-d/4} \det(\operatorname{Im} C_0)^{1/4} \varphi[q_0, p_0, C_0](x), \quad x \in \mathbb{R}^d,$$

the Gaussian amplitude g defined in (2.1), and let $M := C_0 + iG \in \mathbb{C}^{d \times d}$. Moreover, for $q \in \mathbb{R}^d$, define the parameters $p'_0 := p_0 - iG(q - q_0) \in \mathbb{C}$ and

$$\eta := (\pi\varepsilon)^{-d/2} \det(G \operatorname{Im} C_0)^{1/4} \exp\left(-\frac{1}{2\varepsilon} \|q - q_0\|_G^2\right) > 0.$$

Then, both $\Psi g(\bullet - q)$ and its Fourier transform can be expressed in terms of the wave packet φ in (2.11) as

$$(2.12) \quad \begin{aligned} \Psi g(\bullet - q) &= \eta \varphi[q_0, p'_0, M] \quad \text{and} \\ \mathcal{F}_\varepsilon[\Psi g(\bullet - q)] &= \frac{\eta e^{-ip'_0 \cdot q_0 / \varepsilon}}{\sqrt{\det(G - iC_0)}} \varphi[p'_0, -q_0, -M^{-1}], \end{aligned}$$

where the branch of the square root is determined by the requirement that

$$\det(G - iC_0)^{-1/2} > 0,$$

if $G - iC_0$ is real and positiv definite. In particular, for all $(q, p) \in \mathbb{R}^{2d}$ we have

$$(2.13) \quad \langle g_z, \Psi \rangle = (2\pi\varepsilon)^{d/2} e^{ip \cdot q / \varepsilon} \mathcal{F}_\varepsilon[\Psi g(\bullet - q)](p).$$

Proof. For all $x \in \mathbb{R}^d$ we calculate

$$\begin{aligned} \Psi(x) g(x - q) &= (\pi\varepsilon)^{-d/2} \det(G \operatorname{Im} C_0)^{1/4} \dots \\ &\quad \exp\left(\frac{i}{\varepsilon} \left(\frac{1}{2}(x - q_0)^T C_0 (x - q_0) + p_0^T (x - q_0)\right) - \frac{1}{2\varepsilon} (x - q)^T G (x - q)\right). \end{aligned}$$

In particular, for the exponent we obtain

$$\begin{aligned} \frac{i}{2\varepsilon} (x - q_0)^T C_0 (x - q_0) + \frac{i}{\varepsilon} p_0^T (x - q_0) - \frac{1}{2\varepsilon} (x - q)^T G (x - q) &= \dots \\ \frac{i}{2\varepsilon} (x - q_0)^T M (x - q_0) + \frac{1}{2\varepsilon} (\|x - q_0\|_G^2 - \|x - q\|_G^2) + \frac{i}{\varepsilon} p_0^T (x - q_0), \end{aligned}$$

where

$$\|x - q_0\|_G^2 - \|x - q\|_G^2 = 2\langle q - q_0, x - q_0 \rangle_G - \|q - q_0\|_G^2.$$

This implies the identity

$$\frac{1}{2\varepsilon} (\|x - q_0\|_G^2 - \|x - q\|_G^2) + \frac{i}{\varepsilon} p_0^T (x - q_0) = \frac{i}{\varepsilon} p_0'^T (x - q_0) - \frac{1}{2\varepsilon} \|q - q_0\|_G^2,$$

which shows that

$$\Psi g(\bullet - q) = \eta \varphi[q_0, p'_0, M].$$

The formula for the Fourier transform is based on an analytic expression of Gaussian integrals and can be found e.g. in [Fol89, Appendix A, Theorem 2]. Finally, the formula for the inner product follows by the relation in (2.10). \square

In a next step, we turn the Fourier representation of Proposition 2.4 that relies on the functions $\mathcal{I}_q(x)$ in a wave packet representation of the Gaussian wave packet Ψ in terms of Gaussian amplitude functions of unit width. We first calculate an explicit formula for $\mathcal{I}_q(x)$.

Lemma 2.6. *Under the assumptions of Lemma 2.5 we consider a Gaussian wave packet Ψ whose width matrix has the special form $C_0 = iA_0$, where $A_0 \in \mathbb{R}^{d \times d}$ is a real symmetric and positive definite matrix. Moreover, let $A := (G + A_0)^{-1}$ and, for all $x \in \mathbb{R}^d$,*

$$b(x) := x - q + AA_0(q - q_0),$$

$$c(x) := \frac{\det(GA_0)^{1/4}}{(\pi\varepsilon)^d \sqrt{2^d \det(G + A_0)}} \exp\left(-\frac{1}{2\varepsilon} \|q - q_0\|_{GA_0}^2 + \frac{i}{\varepsilon} p_0^T (x - q_0)\right).$$

Then, for all $x \in \mathbb{R}^d$, we have

$$(2.14) \quad \mathcal{I}_q(x) = g(x - q)c(x) \int_{\mathbb{R}^d} \exp\left(-\frac{1}{2\varepsilon} p^T A p + \frac{i}{\varepsilon} b(x)^T p\right) dp.$$

Proof. According to Proposition 2.4, the function \mathcal{I}_q is given for all $x \in \mathbb{R}^d$ by

$$\mathcal{I}_q(x) = (2\pi\varepsilon)^{-d} \int_{\mathbb{R}^d} \langle g_z, \Psi \rangle g_z(x) dp.$$

We combine the connection between the inner product $\langle g_z, \Psi \rangle$ and the Fourier transform $\mathcal{F}_\varepsilon[\Psi g(\bullet - q)]$ in (2.13) with the formula in (2.12), which yields

$$(2\pi\varepsilon)^{-d} \langle g_z, \Psi \rangle g_z(x) = (2\pi\varepsilon)^{-d/2} \mathcal{F}_\varepsilon[\Psi g(\bullet - q)](p) e^{ix \cdot p/\varepsilon} g(x - q)$$

$$= (2\pi\varepsilon)^{-d/2} \left(\frac{\eta e^{-ip'_0 \cdot q_0/\varepsilon}}{\sqrt{\det(G - iC_0)}} \varphi[p'_0, -q_0, -M^{-1}](p) \right) e^{ix \cdot p/\varepsilon} g(x - q).$$

Recalling the definition of $p'_0 = p_0 - iG(q - q_0)$ in Lemma 2.5, we have

$$e^{-ip'_0 \cdot q_0/\varepsilon} \varphi[p'_0, -q_0, -M^{-1}](p) = \varphi[p_0, 0, -M^{-1}](p) \cdots$$

$$\exp\left(-\frac{i}{\varepsilon} (q - AA_0(q - q_0))^T (p - p_0)\right) \exp\left(\frac{1}{2\varepsilon} \|q - q_0\|_{GAG}^2 - \frac{i}{\varepsilon} p_0^T q_0\right),$$

and by definition of $b(x)$ and $c(x)$ we conclude that

$$(2.15) \quad (2\pi\varepsilon)^{-d} \langle g_z, \Psi \rangle g_z(x) = g(x - q)c(x)\varphi[p_0, b(x), -M^{-1}](p).$$

Therefore, (2.14) follows by $A = iM^{-1}$. \square

For simplicity of the formulas we used $C_0 = iA_0$, although any choice for the matrix $C_0 \in \mathbb{C}^{d \times d}$ in the Siegel half-space is also possible and results in similar albeit more involved formulas. If we work with the position grid $\{q_k\}_{k \in \Gamma_q}$, we replace q by q_k and write b_k and c_k instead of b and c . Moreover, for all $k \in \Gamma_q$ and $x \in \mathbb{R}^d$, we introduce the function

$$(2.16) \quad f_{k,x}(p) := \exp\left(-\frac{1}{2\varepsilon} p^T A p + \frac{i}{\varepsilon} b_k(x)^T p\right), \quad p \in \mathbb{R}^d.$$

In particular, (2.15) shows that

$$(2.17) \quad (2\pi\varepsilon)^{-d} \langle g_{(q_k, p_j)}, \Psi \rangle e^{ip_j \cdot (x - q_k)/\varepsilon} = c_k(x) f_{k,x}(p_j - p_0)$$

and therefore, combining Proposition 2.4 and Lemma 2.6, we obtain the following representation of the Gaussian wave packet Ψ :

$$(2.18) \quad \Psi(x) = \frac{1}{S(\Gamma_q; x)} \sum_{k \in \Gamma_q} \left(g(x - q_k) c_k(x) \int_{\mathbb{R}^d} f_{k,x}(p) dp \right), \quad x \in \mathbb{R}^d.$$

At first glance, the representation in (2.18) might appear unfinished, since it still contains a Gaussian integral, which could be solved by hand. Let us discuss in the one-dimensional case, how one uses the representation.

Since $f_{k,x}$ is a Gaussian centered at $p = 0$, we can use a uniform grid $\{p_j\}_{j=1}^N$ on some finite interval $[p_0 - L_p, p_0 + L_p]$ to obtain the approximation

$$(2.19) \quad \int_{\mathbb{R}} f_{k,x}(p) dp \approx \int_{p_0-L_p}^{p_0+L_p} f_{k,x}(p-p_0) dp \approx \sum_{j=1}^N f_{k,x}(p_j-p_0) \Delta p,$$

and therefore, combining the representation in (2.18) with the approximation in (2.19), we get

$$\Psi(x) \approx \frac{1}{S(\Gamma_q; x)} \sum_{k \in \Gamma_q} \sum_{j=1}^N \left(\frac{\Delta p}{2\pi\varepsilon} \langle g_{j,k}, \Psi \rangle \right) g_{j,k}(x),$$

where $g_{j,k} := g_{(q_k, p_j)}$. Note that a direct discretization of the phase space integral in (1.1) with uniform Riemann sums in both position and momentum yields

$$\Psi(x) \approx \frac{\Delta q \Delta p}{2\pi\varepsilon} \sum_{k=1}^M \sum_{j=1}^N \langle g_{j,k}, \Psi \rangle g_{j,k}(x).$$

Consequently, we recognize that the discretization of

$$(2.20) \quad \int_{\mathbb{R}} f_{k,x}(p) dp$$

can be used to obtain a representation, which can be viewed as a discrete version of the FBI transform inversion formula in (1.1). The next section deals with the approximation of the integral in (2.20) via different quadrature rules. The goal is to find rules such that the number of grid points can be kept small. We will see that Gauss–Hermite quadrature is a good candidate, because the integrand $f_{k,x}$ is a Gaussian function.

3. DISCRETIZATION VIA DIFFERENT QUADRATURE RULES

We learn from the previous discussions that a discretization of the integral in (2.20) via quadrature rules yields approximations of the Gaussian wave packet Ψ . In this section, we derive error bounds in 1D for approximations based on

- (TcM) a truncation of the integral, combined with a discretization of the truncated integral by the (compound) midpoint rule;
- (RS) an infinite Riemann sum on a uniform grid;
- (GH) Gauss–Hermite quadrature;

We note that discretizations based on finite uniform grids have been used by Batista et al. (2016) and by Qian and Ying (2010), but to the best of our knowledge, it is the first time that Gauss–Hermite quadrature is used to derive a new variant of the Gaussian wave packet transform. In particular, Gauss–Hermite quadrature can be treated efficiently in moderate dimensions by sparse-grids, see §3.6.

From now on we work with the one-dimensional Gaussian wave packet

$$\Psi(x) = (\pi\varepsilon)^{-1/4} \alpha^{1/4} \exp\left(-\frac{\alpha}{2\varepsilon}(x-q_0)^2 + \frac{i}{\varepsilon}p_0(x-q_0)\right),$$

where $\alpha > 0$ is a width parameter. The parameters in Lemma 2.6 reduce to

$$(3.1) \quad \begin{aligned} A &= \frac{1}{\alpha + \gamma}, \quad b_k(x) = x - q_k + \frac{\alpha}{\alpha + \gamma}(q_k - q_0), \\ c_k(x) &= \frac{(\alpha\gamma)^{1/4}}{\pi\varepsilon\sqrt{2(\alpha + \gamma)}} \exp\left(-\frac{\alpha\gamma}{2\varepsilon(\alpha + \gamma)}(q_k - q_0)^2 + \frac{i}{\varepsilon}p_0(x - q_0)\right). \end{aligned}$$

We are interested in an approximation of $\Psi(x)$ for values x near the center $q_0 \in \mathbb{R}$. Therefore, we consider an interval

$$\Lambda_x = [q_0 - L_q, q_0 + L_q],$$

where $L_q > 0$ is a constant depending on the width α . In the following, we will work with two different position grids: For $\Gamma_q = \{1, \dots, M\}$ we define

$$(3.2) \quad q_k = q_0 - L_q + \frac{2k-1}{2} \cdot \Delta q$$

where $\Delta q = 2L_q/M$ for some $M \geq 1$. Furthermore, for $\Gamma_q = \mathbb{Z}$ and $\Delta q > 0$ we use the uniform infinite grid $q_k = q_0 + k\Delta q$. These two choices imply the following bounds, which will be used later:

Lemma 3.1. *There exists a positive constant $C_{\Gamma_q} > 0$, depending on ε, γ and the choice of the grid $\{q_k\}_{k \in \Gamma_q}$, such that for all $x \in \Lambda_x$ we have*

$$(3.3) \quad \frac{1}{S(\Gamma_q; x)} \sum_{k \in \Gamma_q} g(x - q_k) < C_{\Gamma_q}.$$

In particular, for $\Gamma_q = \{1, \dots, M\}$, the constant is bounded in M and

$$\lim_{M \rightarrow \infty} C_{\Gamma_q} = \frac{2\sqrt{2}(\pi\varepsilon)^{1/4}\gamma^{-1/4}}{\operatorname{erf}(2L_q\sqrt{\frac{\gamma}{\varepsilon}})}.$$

We present the proof in Appendix A. The discretization of the integral in (2.20) via different quadrature rules yields approximations of the Gaussian wave packet

$$\Psi(x) \approx \frac{1}{S(\Gamma_q; x)} \sum_{k \in \Gamma_q} \sum_{j \in \Gamma_p^{(\text{rule})}} r_{j,k}^{(\text{rule})} g_{j,k}(x)$$

that are based on different momentum grids and coefficients. We choose:

For TcM: The finite uniform grid

$$p_j = p_0 - L_p + \frac{2j-1}{2} \cdot \Delta p, \quad j \in \Gamma_p^{(\text{TcM})} = \{1, \dots, N\},$$

with grid size $\Delta p = 2L_p/N$. The representation coefficients

$$r_{j,k}^{(\text{TcM})} = \frac{\Delta p}{2\pi\varepsilon} \langle g_{j,k}, \Psi \rangle$$

can be evaluated by the explicit formula (2.17).

For RS: The infinite uniform grid of size $\Delta p > 0$, i.e.

$$p_j = p_0 + j \cdot \Delta p, \quad j \in \Gamma_p^{(\text{RS})} = \mathbb{Z}.$$

The representation coefficients are given by $r_{j,k}^{(\text{RS})} = r_{j,k}^{(\text{TcM})}$.

For GH: The grid points p_j depend on the zeros s_j of the N th Hermite polynomial and are given by

$$p_j = p_0 + s_j \sqrt{2\varepsilon(\alpha + \gamma)}, \quad j \in \Gamma_p^{(\text{GH})} = \{1, \dots, N\}.$$

The coefficients depend on the shifted nodes w_j of the quadrature rule,

$$r_{j,k}^{(\text{GH})} = \frac{w_j}{2\pi\varepsilon} \langle g_{j,k}, \Psi \rangle,$$

and can also be evaluated by the explicit formula (2.17).

We obtain the following error estimates:

Theorem 3.2 (Gaussian wave packet transform via quadrature rules).

The approximation errors

$$E^{(\text{rule})} := \sup_{x \in \Lambda_x} \left| \Psi(x) - \frac{1}{S(\Gamma_q; x)} \sum_{k \in \Gamma_q} \sum_{j \in \Gamma_p^{(\text{rule})}} r_{j,k}^{(\text{rule})} g_{j,k}(x) \right|$$

for the rules (TcM), (RS) and (GH) satisfy the following bounds:

Truncation and compound midpoint rule: *There exist positive constants $C^{(\text{T})} > 0$ and $C^{(\text{cM})} > 0$ such that*

$$E^{(\text{TcM})} < C^{(\text{T})} + C^{(\text{cM})} \cdot N^{-2}.$$

(Infinite) Riemann sum: *For all $l \geq 1$, there exists a positive constant $C_l^{(\text{RS})} > 0$ such that*

$$E^{(\text{RS})} < C_l^{(\text{RS})} \cdot (\Delta p)^{2l+1}.$$

Gauss–Hermite quadrature: *For all $l \geq 1$, there exists a positive constant $C_r^{(\text{GH})} > 0$ such that*

$$E^{(\text{GH})} < C_l^{(\text{GH})} \cdot N^{-l/2}.$$

The proof is given later and is based on the error estimates for the individual quadrature rules. As we can see, the approximations by the Riemann sum and the Gauss–Hermite quadrature yield spectral convergence, whereas the truncation and midpoint rule result in approximations of order $\mathcal{O}(N^{-2})$. However, we recognize that the representation coefficients for (TcM) and (RS) are equal (which shouldn't be surprising, because both rules are based on uniform grids), and therefore we expect a fast initial decay for the reconstruction error with (TcM). In particular, for smooth and periodic integrands, the midpoint rule achieves spectral accuracy, see e.g. [SI88, Theorem 8], and from a numerical point of view, due to machine tolerance, it can be argued that a computer treats a truncated Gaussian as being periodic for a sufficiently large value of the constant L_p . We will see this effect in our numerical examples in §4. The difference between the representation coefficients of the midpoint rule and the Gauss–Hermite quadrature is the spacing of the grid points p_j on the one hand side, and the different weighting of the inner product $\langle g_{j,k}, \Psi \rangle$ on the other. For the midpoint rule we have to choose the truncation constant L_p , whereas the grid points are distributed “optimally” on the real line for the Gauss–Hermite quadrature. Therefore, we avoid the problem of finding an optimal choice of L_p in the (GH) ansatz.

Remark 3.3. *We note that the approximation of a Gaussian state according to Theorem 3.2 with the (TcM) ansatz can be found in [KMB16], but in contrast to our basis functions $g_{j,k}$, the authors work with the non-normalized functions*

$$(3.4) \quad \phi_{j,k}(x) := \phi(x - q_k) e^{ip_j(x - q_k)}, \quad \phi(x) := \frac{\sqrt{\Delta q}}{\sqrt{\pi}} \frac{\sigma}{2} \exp\left(-\frac{\sigma^2}{4}|x|^2\right),$$

where $\sigma > 0$ is chosen such that $\sigma/2 = \Delta p$. To the best of our knowledge, our error estimate is the first one to apply for the Gaussian representation introduced

by Batista et al.. Combining the basis in (3.4) with uniform grids in position and momentum, the approximation reads

$$\Psi(x) \approx \frac{1}{\sqrt{2\pi}} \sum_{k=1}^M \sum_{j=1}^N \langle \phi_{j,k}, \Psi \rangle \phi_{j,k}(x).$$

3.1. Truncation. Recall the definition of the parameters A and $b_k(x)$ of the integrand $f_{k,x}$ in (2.16). We recognize that $ib_k(x) \cdot p/\varepsilon$ is purely imaginary and therefore the absolute value of $f_{k,x}$ is given for all $p \in \mathbb{R}^d$ by

$$|f_{k,x}(p)| = \exp\left(-\frac{1}{2\varepsilon} p^T A p\right).$$

From a numerical point of view, it is the rapid decay of the integrand which allows us to approximate the improper integral in (2.20) by a (truncated) proper integral. In the next lemma we analyze the corresponding truncation error.

Lemma 3.4 (Truncation).

Recall the definition of the symmetric and positive definite matrix $A \in \mathbb{R}^{d \times d}$ in Lemma 2.6 and denote by $\lambda_j > 0$, $j = 1, \dots, d$ its eigenvalues. Consider the eigendecomposition $A = UDU^T$, where $U \in \mathbb{R}^{d \times d}$ is orthogonal and $D = \text{diag}(\lambda_1, \dots, \lambda_d)$. Moreover, for $L_1, \dots, L_d > 0$ define the set

$$L := \left\{ \sum_{j=1}^d t_j U e_j \mid t_j \in [-L_j, L_j], j = 1, \dots, d \right\},$$

where $e_j \in \mathbb{R}^d$ denotes the j th standard unit vector. Then, for all $k \in \Gamma_q$, we have

$$(3.5) \quad \sup_{x \in \mathbb{R}^d} \left| \int_{\mathbb{R}^d} f_{k,x}(p) dp - \int_L f_{k,x}(p) dp \right| \leq \frac{(2\pi\varepsilon)^{d/2}}{\sqrt{\det A}} \exp\left(-\frac{1}{2\varepsilon} \sum_{j=1}^d \lambda_j L_j^2\right).$$

Proof. Let $k \in \Gamma_q$. Using the eigendecomposition of A we obtain

$$\begin{aligned} \sup_{x \in \mathbb{R}^d} \left| \int_{\mathbb{R}^d} f_{k,x}(p) dp - \int_L f_{k,x}(p) dp \right| &\leq \int_{\mathbb{R}^d \setminus L} \exp\left(-\frac{1}{2\varepsilon} (U^T p)^T D (U^T p)\right) dp \\ &= \int_{\mathbb{R}^d \setminus U^T L} \exp\left(-\frac{1}{2\varepsilon} y^T D y\right) dy, \end{aligned}$$

where the transformed set $U^T L$ is given by

$$U^T L = U^{-1} L = [-L_1, L_1] \times \dots \times [-L_d, L_d].$$

Hence, the symmetry of the integral and Fubini's theorem yields that

$$\int_{\mathbb{R}^d \setminus U^T L} \exp\left(-\frac{1}{2\varepsilon} y^T D y\right) dy = \prod_{j=1}^d 2 \int_{L_j}^{\infty} e^{-\frac{\lambda_j}{2\varepsilon} y_j^2} dy_j.$$

We use the exponential-type bound $\text{erfc}(z) \leq e^{-z^2}$, $z > 0$, for the complementary error function, see e.g. [CDS03, Eq. (5)]. Hence, for $j = 1, \dots, d$ we conclude that

$$2 \int_{L_j}^{\infty} e^{-\frac{\lambda_j}{2\varepsilon} y_j^2} dy_j = \frac{\sqrt{2\pi\varepsilon}}{\sqrt{\lambda_j}} \text{erfc}\left(\sqrt{\lambda_j/2\varepsilon} L_j\right) \leq \frac{\sqrt{2\pi\varepsilon}}{\sqrt{\lambda_j}} \exp\left(-\frac{\lambda_j}{2\varepsilon} L_j^2\right),$$

which yields the following bound:

$$\prod_{j=1}^d 2 \int_{L_j}^{\infty} e^{-\lambda_j y_j^2} dy_j \leq \frac{(2\pi\varepsilon)^{d/2}}{\sqrt{\det A}} \exp\left(-\frac{1}{2\varepsilon} \sum_{j=1}^d \lambda_j L_j^2\right).$$

□

3.2. Estimates for the Integrand. The error bounds of the quadrature rules crucially depend on the smoothness of the integrand. It is therefore useful to have an explicit formula for the bounds of the higher order derivatives of $f_{k,x}$:

Lemma 3.5. *For all $k \in \Gamma_q$, all $x \in \Lambda_x$ and all $p \in \mathbb{R}$, the second derivative of the integrand $f_{k,x}$ is bounded by*

$$(3.6) \quad |f''_{k,x}(p)| \leq e^{-Ap^2/2\varepsilon} \left((2L_q + A|p|)^2 \varepsilon^{-2} + A\varepsilon^{-1} \right).$$

Moreover, for all $l \geq 1$, there exists a positive constant $c_{l,L_q} > 0$, depending on $l, L_q, \varepsilon, \alpha$ and γ , such that for all $k \in \Gamma_q$ we have

$$\sup_{x \in \Lambda_x} \|f_{k,x}^{(l)}\|_{L^1(\mathbb{R})} \leq c_{l,L_q}.$$

Proof. Let $l \geq 1$. As it is presented in [DLCS00, Eq. (13)], for $\alpha, \beta \in \mathbb{C}, \alpha \neq 0$, the l th derivative of the exponential function $U: \mathbb{R} \rightarrow \mathbb{C}$,

$$U(p) := e^{\alpha p^2 + \beta p} \quad \text{for all } p \in \mathbb{R},$$

can be expressed in terms of the second order Kampé de Fériét polynomial as

$$U^{(l)}(p) = U(p) l! \sum_{m=0}^{\lfloor l/2 \rfloor} \frac{\alpha^m (2\alpha p + \beta)^{l-2m}}{m! (l-2m)!}.$$

Hence, if we chose $\alpha = -A/2\varepsilon$ and $\beta = ib_k(x)/\varepsilon$, we conclude that $U(p) = f_{k,x}(p)$. Consequently, for all $k \in \Gamma_q$, all $x \in \Lambda_x$ and all $p \in \mathbb{R}$ we obtain

$$|f_{k,x}^{(l)}(p)| \leq e^{-Ap^2/2\varepsilon} l! \sum_{m=0}^{\lfloor l/2 \rfloor} \frac{A^m (A|p| + 2L_q)^{l-2m}}{2^m \varepsilon^{l-m} m! (l-2m)!},$$

where we used that

$$(3.7) \quad \sup_{x \in \Lambda_x} |b_k(x)| = \frac{1}{\alpha + \gamma} \sup_{x \in \Lambda_x} |\alpha(x - q_0) + \gamma(x - q_k)| \leq 2L_q.$$

Hence, setting $l = 2$ shows (3.6) and it remains to prove the bound for the L^1 -norm. Using the binomial theorem we obtain

$$\|f_{k,x}^{(l)}\|_{L^1(\mathbb{R})} \leq \frac{l!}{\varepsilon^l} \sum_{m=0}^{\lfloor l/2 \rfloor} \frac{A^m \varepsilon^m}{2^m m!} \sum_{n=0}^{l-2m} \frac{A^n (2L_q)^{l-2m-n}}{n! (l-2m-n)!} \int_{\mathbb{R}} |p|^n e^{-Ap^2/2\varepsilon} dp,$$

where the integral can be transformed as

$$\int_{\mathbb{R}} |p|^n e^{-Ap^2/2\varepsilon} dp = (A/\varepsilon)^{-(n+1)/2} \int_{\mathbb{R}} |t|^n e^{-t^2/2} dt.$$

Using the formula for the moments of the normal distribution, see [PP02, Eq. 5-73], we further conclude that

$$M_n := \int_{\mathbb{R}} |t|^n e^{-t^2/2} dt = \begin{cases} \sqrt{2\pi} (n-1)!!, & \text{if } n = 2k, \\ 2^{k+1} k!, & \text{if } n = 2k+1. \end{cases}$$

Hence, using that M_n is an increasing function in n and $M_n/n! \leq 2$ for all $n \geq 1$, we obtain

$$\begin{aligned} \|f_{k,x}^{(l)}\|_{L^1(\mathbb{R})} &\leq \frac{l!}{\varepsilon^l} \sum_{m=0}^{\lfloor l/2 \rfloor} \frac{A^{m-1/2} \varepsilon^{m+1/2}}{2^m m!} \sum_{n=0}^{l-2m} \frac{A^{n/2} \varepsilon^{n/2} (2L_q)^{l-2m-n}}{n! (l-2m-n)!} M_n \\ &= \frac{l!}{\varepsilon^l} \sum_{m=0}^{\lfloor l/2 \rfloor} \frac{A^{m-1/2} \varepsilon^{m+1/2}}{2^m m!} \frac{M_{l-2m}}{(l-2m)!} \left(\sqrt{A\varepsilon} + 2L_q \right)^{l-2m} \\ &\leq \frac{l!}{\varepsilon^l} \sum_{m=0}^{\lfloor l/2 \rfloor} \frac{A^{m-1/2} \varepsilon^{m+1/2}}{2^{m-1} m!} \left(\sqrt{A\varepsilon} + 2L_q \right)^{l-2m}. \end{aligned}$$

□

In the next step, we approximate the truncated integral in Lemma 3.4 using the composite midpoint rule.

3.3. Compound Midpoint Rule and Infinite Riemann Sum. The discretization with the composite midpoint rule yields an approximation of the form

$$(3.8) \quad \int_{-L_p}^{L_p} f_{k,x}(p) \, dp \approx \Delta p \sum_{j=1}^N f_{k,x}(p_j),$$

where $N \geq 1$ is the number of grid points. The next lemma shows that the approximation error is of order $\mathcal{O}(N^{-2})$ as $N \rightarrow \infty$:

Lemma 3.6. *There exists a positive constant $c_{L_p, L_q}^{(\text{cM})} > 0$, depending on L_p, L_q and $\varepsilon, \alpha, \gamma$, such that for all $k \in \Gamma_q$ we have*

$$\sup_{x \in \Lambda_x} \left| \int_{-L_p}^{L_p} f_{k,x}(p) \, dp - \Delta p \sum_{j=1}^N f_{k,x}(p_j) \right| \leq c_{L_p, L_q}^{(\text{cM})} \cdot N^{-2}.$$

Proof. Let $k \in \Gamma_q$ and $x \in \mathbb{R}$. By Lemma 3.5, the integrand is twice differentiable. Thus, as it can be found e.g. in [DR07, chapter 2.1], the error of the composite midpoint rule is bounded by

$$\left| \int_{-L_p}^{L_p} f_{k,x}(p) \, dp - \Delta p \sum_{j=1}^N f_{k,x}(p_j) \right| \leq \frac{L_p^3}{24} \sup_{p \in [-L_p, L_p]} |f_{k,x}''(p)| \cdot N^{-2}.$$

Moreover, the formula for $|f_{k,x}''(p)|$ in (3.6) yields for all $x \in \Lambda_x$:

$$\sup_{p \in [-L_p, L_p]} |f_{k,x}''(p)| \leq \left((2L_q + AL_p)^2 \varepsilon^{-2} + A\varepsilon^{-1} \right).$$

Consequently, the claim follows for the constant

$$(3.9) \quad c_{L_p, L_q}^{(\text{cM})} = \frac{L_p^3}{24} \left((2L_q + AL_p)^2 \varepsilon^{-2} + A\varepsilon^{-1} \right).$$

□

We notice that

$$c_{L_p, L_q}^{(\text{cM})} = \mathcal{O}(L_p^5 + L_q^2).$$

In particular, the asymptotic behavior in L_p underlines the importance, that the truncation parameter must not be chosen too large for the (TcM) ansatz.

In addition to an approximation of the truncated integral with the midpoint rule as presented in Lemma 3.6, we can also use an infinite Riemann sum on a uniform

grid to approximate the improper integral directly, without truncation. The error estimate for this approximation is based on the Euler-Maclaurin formula:

Lemma 3.7. *Let $\{p_j\}_{j \in \mathbb{Z}}$ be a uniform grid with size $\Delta p > 0$. Then, for all $l \geq 1$, there exists a positive constant $c_{l, L_q}^{(\text{RS})} > 0$, depending on l, L_q and $\varepsilon, \alpha, \gamma$, such that for all $k \in \Gamma_q$ we have*

$$\sup_{x \in \Lambda_x} \left| \int_{\mathbb{R}} f_{k,x}(p) dp - \Delta p \sum_{j \in \mathbb{Z}} f_{k,x}(p_j) \right| \leq c_{l, L_q}^{(\text{RS})} \cdot (\Delta p)^{2l+1}.$$

Proof. Let $l \geq 1$. Since the integrand $f_{k,x}$ is a Gaussian function, we can use the Euler-Maclaurin formula, see e.g. [KU98, Theorem 7.2.1], to obtain for all $k \in \Gamma_q$ and all $x \in \Lambda_x$:

$$\left| \int_{\mathbb{R}} f_{k,x}(p) dp - \Delta p \sum_{j \in \mathbb{Z}} f_{k,x}(p_j) \right| \leq \frac{\|f_{k,x}^{(2l+1)}\|_{L^1(\mathbb{R})}}{(2\pi)^{2l+1}} \cdot (\Delta p)^{2l+1}.$$

By Lemma 3.5, there is a positive constant $c_{l, L_q} > 0$, depending on l, L_q and $\varepsilon, \alpha, \gamma$, such that for all $k \in \Gamma_q$:

$$\sup_{x \in \Lambda_x} \|f_{k,x}^{(2l+1)}\|_{L^1(\mathbb{R})} \leq c_{l, L_q}.$$

Hence, the claim follows for $c_{l, L_q}^{(\text{RS})} = c_{l, L_q} / (2\pi)^{2l+1}$. \square

3.4. Gauss–Hermite Quadrature. We now use Gauss–Hermite quadrature for the approximation of the integral, which is a special form of Gaussian quadrature on the real line for a Gaussian weight function, see e.g. [DR07, 3.6.11]. Using the quadrature rule with $N \geq 1$ nodes, the linear transformation $s = p / \sqrt{2\varepsilon(\alpha + \gamma)}$ in the integrand yields

$$(3.10) \quad \int_{\mathbb{R}} f_{k,x}(p) dp \approx \sqrt{2\varepsilon(\alpha + \gamma)} \sum_{j=1}^N \omega_j e^{s_j^2} f_{k,x}(s_j \sqrt{2\varepsilon(\alpha + \gamma)}),$$

where the quadrature nodes s_1, \dots, s_N are chosen as the zeros of the N th Hermite polynomial and the real numbers ω_j are the corresponding nodes. In particular, the N th Hermite polynomial and the weights are given by

$$H_N(x) = (-1)^N e^{x^2} \frac{d^N}{dx^N} e^{-x^2} \quad \text{and} \quad \omega_j = \frac{2^{N+1} N! \sqrt{\pi}}{[H_{N+1}(s_j)]^2}.$$

The weights and the nodes depend on N , but we do not indicate this dependence in our notation. Using the transformed nodes and weights

$$(3.11) \quad p_j = s_j \sqrt{2\varepsilon(\alpha + \gamma)} \quad \text{and} \quad w_j = \sqrt{2\varepsilon(\alpha + \gamma)} \omega_j e^{s_j^2},$$

we can rewrite the approximation in (3.10) in the more handy form

$$\int_{\mathbb{R}} f_{k,x}(p) dp \approx \sum_{j=1}^N w_j f_{k,x}(p_j).$$

For this approximation we obtain the following error bound:

Lemma 3.8. *Let the transformed nodes p_j and weights w_j be defined as in (3.11). Then, for all $l \geq 1$, there exists a positive constant $c_{l, L_q}^{(\text{GH})} > 0$, depending on l, L_q and $\varepsilon, \alpha, \gamma$, such that for all $k \in \Gamma_q$ we have*

$$(3.12) \quad \sup_{x \in \Lambda_x} \left| \int_{\mathbb{R}} f_{k,x}(p) dp - \sum_{j=1}^N w_j f_{k,x}(p_j) \right| \leq c_{l, L_q}^{(\text{GH})} \cdot N^{-l/2}.$$

Proof. Let $k \in \Gamma_q$ and $x \in \Lambda_x$. By a linear transformation we obtain

$$\int_{\mathbb{R}} f_{k,x}(p) dp = \sqrt{2\varepsilon(\alpha + \gamma)} \int_{\mathbb{R}} e^{-s^2} h_{k,x}(s) ds,$$

where the complex-valued function $h_{k,x}: \mathbb{R} \rightarrow \mathbb{C}$ is given for all $s \in \mathbb{R}$ by

$$h_{k,x}(s) := \exp\left(ib_k(x)s\sqrt{\frac{2(\alpha + \gamma)}{\varepsilon}}\right).$$

In particular, for $l \geq 1$, the l th derivative is bounded by

$$|h_{k,x}^{(l)}(s)| = 2^{l/2}(\alpha + \gamma)^{l/2}\varepsilon^{-l/2}|b_k(x)|^l \leq 2^{3l/2}(\alpha + \gamma)^{l/2}\varepsilon^{-l/2}L_q^l,$$

where we used the estimate in (3.7). In [MM94, Theorem 2], the authors prove that if the $(l - 1)$ th derivative of a function $g: \mathbb{R} \rightarrow \mathbb{C}$ is locally absolutely continuous and $g^{(l)}(s)e^{-(1-\delta)s^2} \in L^1(\mathbb{R})$ for some $l \geq 1$ and $0 < \delta < 1$, then

$$\left| \int_{\mathbb{R}} e^{-s^2} g(s) ds - \sum_{j=1}^N \omega_j g(s_j) \right| \leq C \cdot N^{-l/2} \|g^{(l)}(s)e^{-(1-\delta)s^2}\|_{L^1(\mathbb{R})},$$

where C is a constant independent of N and g . Since for all $l \geq 1$ and all $0 < \delta < 1$ we have $h_{k,x}^{(l)}(s)e^{-(1-\delta)s^2} \in L^1(\mathbb{R})$ with L^1 -norm

$$\|h_{k,x}^{(l)}(s)e^{-(1-\delta)s^2}\|_{L^1(\mathbb{R})} \leq 2^{3l/2}(\alpha + \gamma)^{l/2}\varepsilon^{-l/2}L_q^l \sqrt{\frac{\pi}{1-\delta}},$$

we obtain the following bound:

$$\sup_{x \in \Lambda_x} \left| \int_{\mathbb{R}} e^{-s^2} h_{k,x}(s) ds - \sum_{j=1}^N \omega_j h_{k,x}(s_j) \right| \leq C \cdot N^{-l/2} \cdot 2^{3l/2}(\alpha + \gamma)^{l/2}\varepsilon^{-l/2}L_q^l \sqrt{\pi}.$$

Consequently, (3.12) follows for

$$c_{l,L_q}^{(\text{GH})} = C \cdot 2^{(3l+1)/2}(\alpha + \gamma)^{(l+1)/2}\varepsilon^{-(l-1)/2}L_q^l \sqrt{\pi}.$$

□

3.5. Proof of the Final Result. We are now ready to present the proof for the approximation errors in Theorem 3.2:

(*Proof of Theorem 3.2*). Let $x \in \Lambda_x$. Using the representation of the Gaussian wave packet Ψ according to Proposition 2.4, we calculate

$$E^{(\text{rule})} \leq \frac{1}{S(\Gamma_q; x)} \sum_{k \in \Gamma_q} \left| \mathcal{I}_{q_k}(x) - \sum_{j \in \Gamma_p^{(\text{rule})}} r_{j,k}^{(\text{rule})} g_{j,k}(x) \right|.$$

We are now considering rule = TcM. Combining the representation of Ψ according to Lemma 2.6 with the truncation and the compound midpoint rule, we obtain

$$\begin{aligned} \mathcal{I}_{q_k}(x) &\stackrel{(2.14)}{=} c_k(x)g(x - q_k) \int_{\mathbb{R}^d} f_{k,x}(p) dp \\ &\stackrel{(3.5)}{\approx} c_k(x)g(x - q_k) \int_{-L_p}^{L_p} f_{k,x}(p) dp \quad (\text{truncation}) \\ &\stackrel{(3.8)}{\approx} \sum_{j=1}^N r_{j,k}^{(\text{TcM})} g_{j,k}(x) \quad (\text{compound midpoint rule}), \end{aligned}$$

where the representation coefficients $r_{j,k}^{(\text{TcM})} \in \mathbb{C}$ are given by

$$r_{j,k}^{(\text{TcM})} = \Delta p \cdot c_k(x) f_{k,x}(p_j - p_0) e^{-ip_j(x-q_k)/\varepsilon} \stackrel{(2.17)}{=} \frac{\Delta p}{2\pi\varepsilon} \langle g_{j,k}, \Psi \rangle.$$

Hence, for all $j \in \{1, \dots, N\}$ and all $k \in \Gamma_q$, we obtain

$$\left| \mathcal{I}_{q_k}(x) - \sum_{j=1}^N r_{j,k}^{(\text{TcM})} g_{j,k}(x) \right| = |c_k(x)| g(x - q_k) \left| \int_{\mathbb{R}} f_{k,x}(p) dp - \Delta p \sum_{j=1}^N f_{k,x}(p_j) \right|.$$

Furthermore, it follows by the definition of $c_k(x)$ in (3.1) that

$$|c_k(x)| = \frac{(\alpha\gamma)^{1/4}}{\pi\varepsilon\sqrt{2(\alpha+\gamma)}} \exp\left(-\frac{\alpha\gamma}{2\varepsilon(\alpha+\gamma)}(q_k - q_0)^2\right) \leq \frac{(\alpha\gamma)^{1/4}}{\pi\varepsilon\sqrt{2\pi(\alpha+\gamma)}}.$$

By Lemma 3.4 (truncation) and Lemma 3.6 (compound midpoint rule), we conclude that there are positive constants $c_{L_p}^{(\text{T})} > 0$ and $c_{L_p, L_q}^{(\text{cM})} > 0$, respectively, such that

$$\left| \int_{\mathbb{R}} f_{k,x}(p) dp - \Delta p \sum_{j=1}^N f_{k,x}(p_j) \right| \leq c_{L_p}^{(\text{T})} + c_{L_p, L_q}^{(\text{cM})} \cdot N^{-2}.$$

Lemma 3.1 yields the existence of a constant $C_{\Gamma_q} > 0$ such that

$$\frac{1}{S(\Gamma_q; x)} \sum_{k \in \Gamma_q} g(x - q_k) < C_{\Gamma_q}, \quad x \in \Lambda_x.$$

Hence, we conclude that

$$\begin{aligned} & \frac{1}{S(\Gamma_q; x)} \sum_{k \in \Gamma_q} \left| \mathcal{I}_{q_k}(x) - \sum_{j=1}^N r_{j,k}^{(\text{TcM})} g_{j,k}(x) \right| \\ & \leq \frac{(\alpha\gamma)^{1/4}}{\pi\varepsilon\sqrt{2(\alpha+\gamma)}} \left(c_{L_p}^{(\text{T})} + c_{L_p, L_q}^{(\text{cM})} \cdot N^{-2} \right) \frac{1}{S(\Gamma_q; x)} \sum_{k \in \Gamma_q} g(x - q_k) \\ & < C^{(\text{T})} + C^{(\text{cM})} \cdot N^{-2}, \end{aligned}$$

where the positive constants $C^{(\text{T})}, C^{(\text{cM})} > 0$ are given by

$$C^{(\text{T})} = \frac{(\alpha\gamma)^{1/4}}{\pi\varepsilon\sqrt{2(\alpha+\gamma)}} c_{L_p}^{(\text{T})} C_{\Gamma_q} \quad \text{and} \quad C^{(\text{cM})} = \frac{(\alpha\gamma)^{1/4}}{\pi\varepsilon\sqrt{2(\alpha+\gamma)}} c_{L_p, L_q}^{(\text{cM})} C_{\Gamma_q}.$$

The corresponding estimates for the infinite Riemann sum and Gauss–Hermite quadrature follow the same arguments as presented for (TcM), but using Lemma 3.7 and Lemma 3.8, respectively. \square

3.6. High-dimensional Quadrature. For the discretization of the multidimensional Gaussian integral

$$\int_{\mathbb{R}^d} f_{k,x}(p) dp = \int_{\mathbb{R}^d} \exp\left(-\frac{1}{2\varepsilon} p^T A p + \frac{i}{\varepsilon} b_k(x)^T p\right) dp$$

conventional grid based approaches such as Riemann sums or one-dimensional Gauss–Hermite quadrature in every coordinate direction are unacceptably slow and no longer practical, since the number of function evaluations increases exponentially with the dimension d , see e.g. [KU98, chapter 6]. Sparse grid methods can overcome this curse of dimension to a certain extent. We refer to [GG98] for a comprehensive presentation of several methods based on Smolyak’s sparse grid construction and further developments. In particular, sparse grids have been used for the midpoint rule, see [BD93], and for Gauss–Hermite quadrature, see [LL20, chapter 8.1]. For the latter, the costs of the discretization are vastly reduced and thus enables

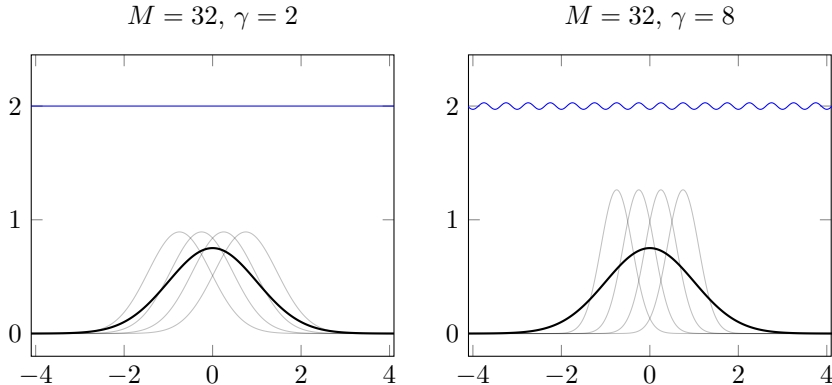


FIGURE 2. Plot of the wave packet Ψ (black), four basis functions around the center $q_0 = 0$ (gray) and the summation curve (blue) for two choices of the width parameter γ . According to Lemma 2.1, the summation curve can be approximated by the constant $1/\Delta q = 2$. The smaller value of γ (left) yields a better approximation.

the generalization of the Gaussian wave packet transform based on Gauss–Hermite quadrature. Indeed, this variant needs less than $K(\log K)^{d-1}$ quadrature nodes, whereas K^d are required for the full tensor grid, and an error bound for this approximation can be found in [LL20, Theorem 8.2]. We note that there is a large variety of other methods that can be used such as Monte Carlo and Quasi-Monte Carlo methods, see e.g. [Nie92]. The discretization with these methods allow to derive new variants of the Gaussian wave packet transform and can potentially be used in higher dimensions.

4. NUMERICAL RESULTS

We present numerical experiments for the reconstruction of one-dimensional Gaussian wave packets according to Theorem 3.2. In comparison to representations that are based on uniform grids such as (TcM), the different setups shall illustrate the superiority of our new representation obtained by Gauss–Hermite quadrature. We focus on two examples to demonstrate the dependence of the reconstruction errors on the various parameters that are involved. The first example deals with the interplay of the parameters $\gamma > 0$ (width of the basis functions) and $M \geq 1$ (number of grid points in position space), while in the second example we study the dependence on the semiclassical parameter $\varepsilon > 0$, which controls the oscillations of both the wave packet Ψ and of the basis functions $g_{j,k}$.

4.1. Example 1. We consider the wave packet

$$\Psi(x) = \pi^{-1/4} \exp\left(-\frac{1}{2}x^2\right), \quad \left[\varepsilon = 1, \alpha = 1, (q_0, p_0) = (0, 0)\right],$$

on the interval $\Lambda_x = [-8, 8]$. We note that the choice of Λ_x corresponds to $L_q = 8$. The plots in Figure 2 show the wave packet Ψ together with four basis functions around the center $q_0 = 0$ (gray) and the summation curve (blue) for $\gamma = 2$ (left) and $\gamma = 8$ (right). In both plots, the summation curve is built on a uniform grid with $M = 32$ grid points, which gives a spacing of $\Delta q = 0.5$ for the basis functions. Recall that according to Lemma 2.1 the summation curve is Δq -periodic and can be approximated by the constant value $1/\Delta q$.

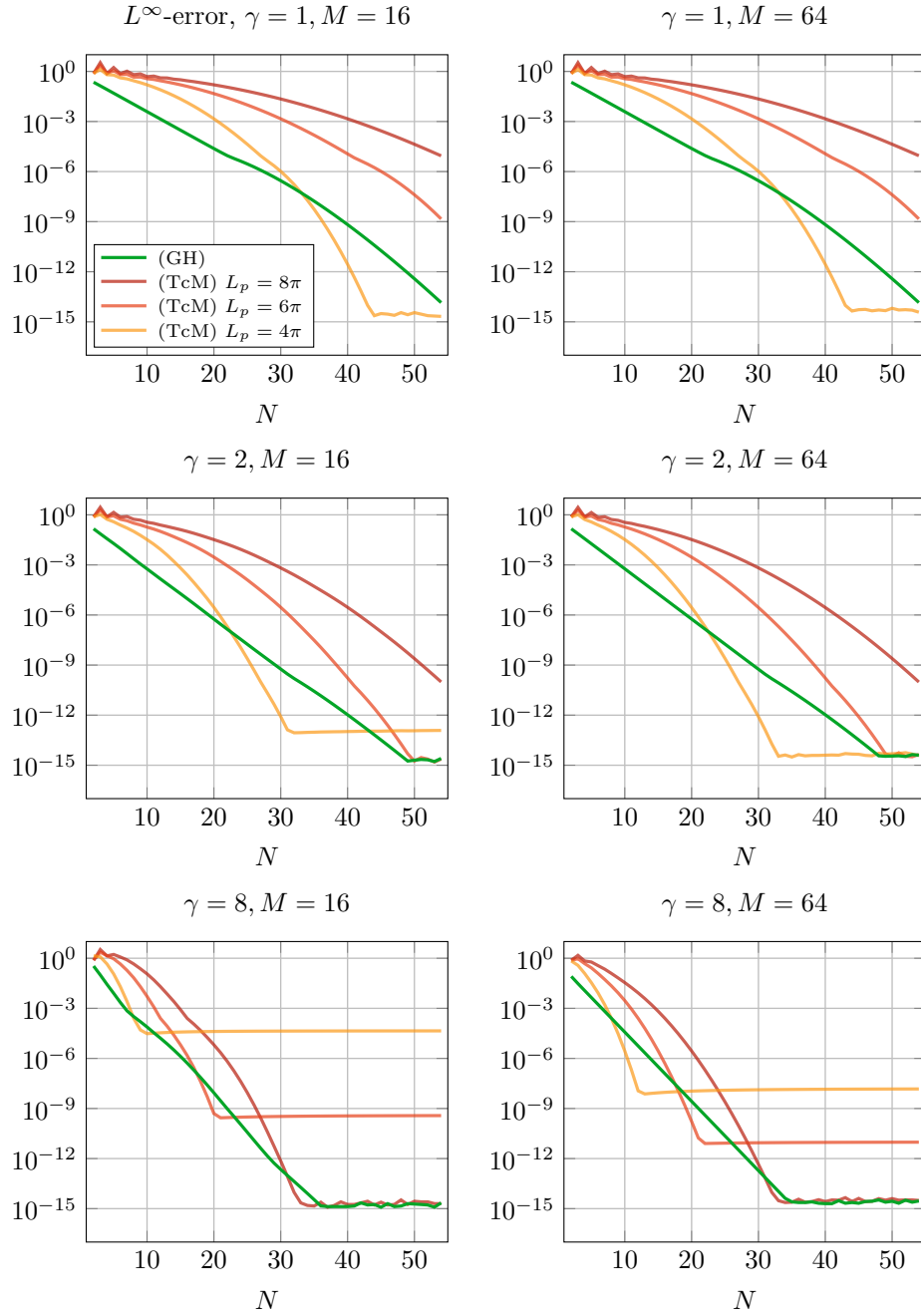


FIGURE 3. Reconstruction errors in the sup-norm for different combinations of M and γ . The approximations with (TcM) have a fast initial decay, followed by a transition to the lower rate (e.g. light red and orange lines in the last row). For (GH) all plots show initial exponential decay (green lines).

In particular, smaller values of γ yield that the variance (and thus the overlap) of the basis functions is getting larger and therefore we obtain better approximations. This can also be observed in the plots: For the summation curve at the right hand side we see the typical oscillations as we know them from the cosine function, whereas at the left hand side no oscillations can be recognized and the summation curve approximates the predicted value $1/\Delta q = 2$ very well. However, we note that for the reconstruction of the wave packet we do not need the approximation of the summation curve. The plots in Figure 3 show the reconstruction errors in the supremum norm on the interval Λ_x for different combinations of the parameters γ and M . For each of the three rows (γ is fixed here) we compare the two numbers $M = 16$ (left) and $M = 64$ (right) of grid points in position space, as well as three choices for the truncation parameter in momentum space ($L_p = 4\pi, 6\pi, 8\pi$). For the (TcM) representations we observe that larger values of L_p yield a worse decay of the error, which is in accordance with our theoretical result in Lemma 3.6. As we learned from the discussions in section 3.3, for (TcM) we expect a fast initial decay, followed by the $\mathcal{O}(N^{-2})$ rate. The transition to the lower rate can be observed e.g. at $N \approx 10$ for the orange line in the last plot on the left hand side ($\gamma = 8, M = 16$). Furthermore, a comparison of the two columns in Figure 3 shows that the error is only slightly effected by the number of grid points in position space (left: $M = 16$, right: $M = 64$). This can be explained by the fact, that all error constants in Theorem 3.2 consist of the independent prefactor $C_{\Gamma_q} > 0$, which stays bounded as $M \rightarrow \infty$ according to Lemma 3.1. For all reconstructions based on Gauss–Hermite quadrature (green lines), the errors show initial exponential decay. We note that Lemma 3.8 predicts spectral convergence for (GH). In particular, in all plots we observe the superiority of (GH) for small numbers N . We notice that already a few grid points are sufficient to get good approximations with the Gauss–Hermite rule. As we will see in the next example, the discrepancy between (TcM) and (GH) becomes even bigger, if the underlying wave packet Ψ is oscillatory.

4.2. Example 2. For $\varepsilon \in \{0.1, 0.05\}$ we consider the wave packet

$$\Psi(x) = (\pi\varepsilon)^{-1/4} \exp\left(-\frac{1}{2\varepsilon}(x-1)^2 + \frac{2i}{\varepsilon}(x-1)\right), \quad \left[\alpha = 1, (q_0, p_0) = (1, 2)\right],$$

on $\Lambda_x = [-8, 8]$. In combination with small values of the semiclassical parameter ε , the presence of the complex phase factor yields that the real and imaginary part of the wave packet is oscillatory, see Figure 4. For all computations we used $M = 128$ points in the position space, corresponding to a uniform spacing of $\Delta q = 1/8$. Moreover, we used two values for the width of the basis functions ($\gamma = 16$ and $\gamma = 32$). For $\varepsilon = 0.1$ and each choice of γ , a plot of four basis functions and the summation curve can be found in Figure 5. As we discussed in the first example, the smaller value of γ (left) yields a better approximation of the summation curve to the constant value $1/\Delta q = 8$. The errors for the reconstruction of the wave packets can be found in Figure 6. As in the first example, we observe that the reconstructions based on Gauss–Hermite quadrature give an initial exponential decay (green lines). For the approximations with (TcM) we recognize that the errors stay constant up to a certain threshold, depending on the value of ε . For instance, as we can see in the plot in the lower left corner ($\varepsilon = 0.05, \gamma = 16, M = 128$), all (TcM) approximations with less than $N = 10$ grid points are unusable. In addition, all plots underline the superiority of the reconstructions based on (GH) for the approximation of a wave packet with high oscillations, independently of the width of the basis functions. Consequently, the experiment shows that using our new reconstruction formula, the number N of grid points can be reduced significantly if the wave packet is highly oscillatory.

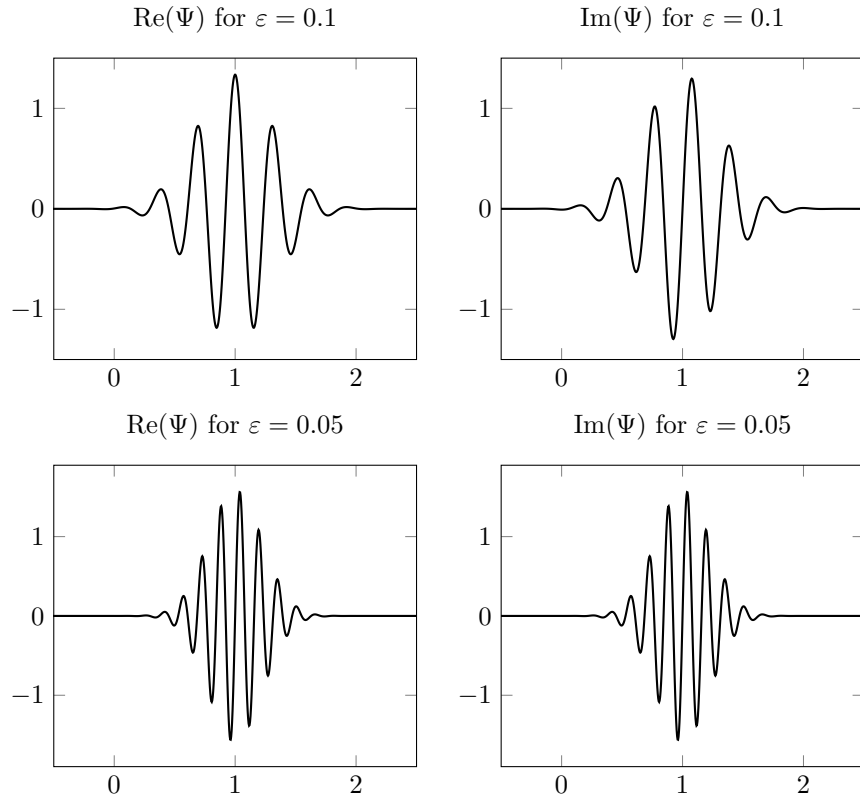


FIGURE 4. Real and imaginary part of the wave packet Ψ for different values of ε . Smaller values yield higher oscillations.

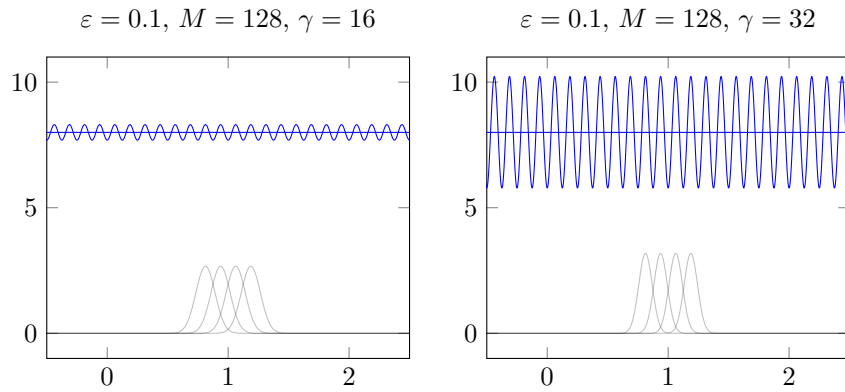


FIGURE 5. Plot of four basis functions (gray) and the summation curve (blue). For the larger value of γ (right), the summation curve highly oscillates around the value $1/\Delta q = 8$.

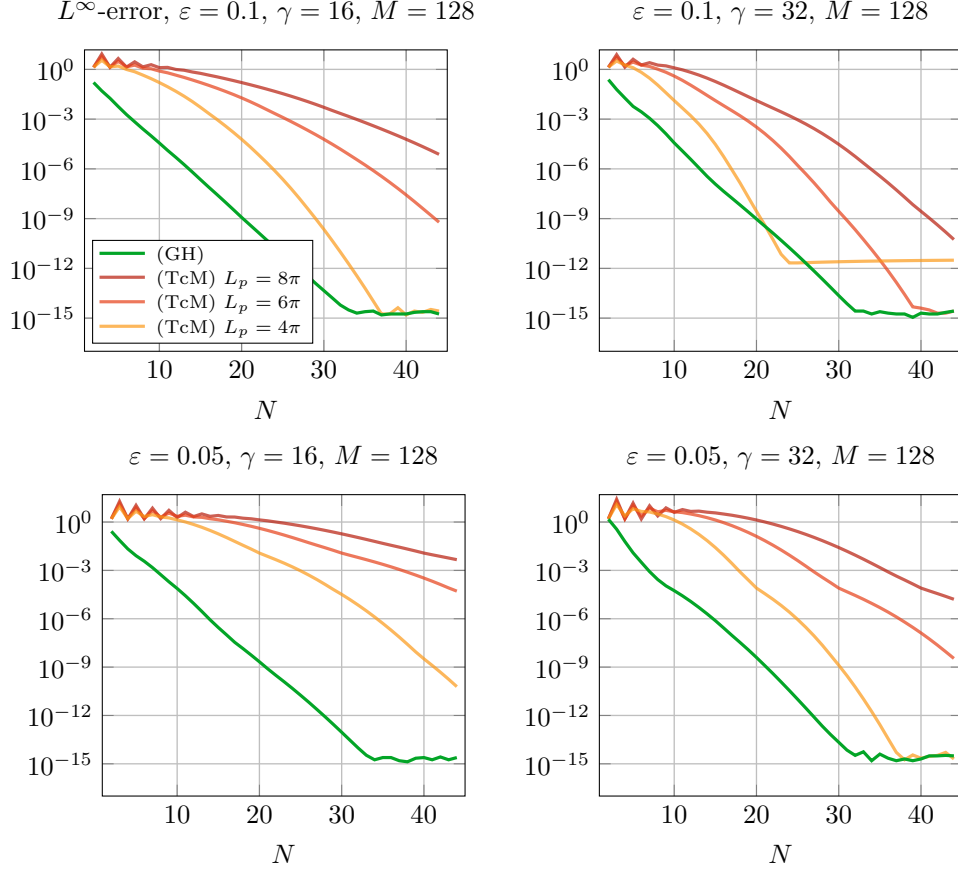


FIGURE 6. Reconstruction errors for different values of γ and ε . The approximations based on Gauss–Hermite quadrature (green) show the best decay. Compared to the midpoint rule, the number of grid points can be reduced significantly with (GH), especially for small values of ε (high oscillations).

APPENDIX A. SUMMATION CURVE

Using a convolution of an unshifted Gaussian with a Dirac comb, it is proven in [ML01, Appendix A] that, for $\Delta q > 0, T > 0$ and all $x \in \mathbb{R}$, we have

$$(A.1) \quad \sum_{k \in \mathbb{Z}} \frac{\Delta q}{T\sqrt{\pi}} \exp\left(-\frac{(x - k \cdot \Delta q)^2}{T^2}\right) = 1 + 2 \sum_{n=1}^{\infty} \cos\left(\frac{2\pi n x}{\Delta q}\right) \exp\left(-\left(\frac{\pi n T}{\Delta q}\right)^2\right),$$

where the convergence is uniform in x . We use this expansion to prove Lemma 2.1:

Proof (of Lemma 2.1). Let $x \in \mathbb{R}$. Using formula (A.1) for $T = \sqrt{\varepsilon/\gamma}$, we obtain

$$\sum_{k \in \mathbb{Z}} \frac{\sqrt{\gamma}}{\sqrt{\pi\varepsilon}} \exp\left(-\frac{\gamma}{\varepsilon}(x - q_k)^2\right) = \frac{1}{\Delta q} \left(1 + 2 \sum_{n=1}^{\infty} \cos\left(\frac{2\pi n x}{\Delta q}\right) \exp\left(-\frac{\pi^2 n^2 \varepsilon}{\gamma(\Delta q)^2}\right)\right),$$

which establishes equation (2.3). Let $r := \exp(-\pi^2\varepsilon/\gamma(\Delta q)^2) < 1$. We then get

$$\begin{aligned} \left| S(\Gamma_q; x) - \frac{1}{\Delta q} \right| &\leq \frac{2}{\Delta q} \sum_{n=1}^{\infty} \left| \cos\left(\frac{2\pi n x}{\Delta q}\right) \exp\left(-\frac{\pi^2 n^2 \varepsilon}{\gamma(\Delta q)^2}\right) \right| \\ &\leq \frac{2}{\Delta q} \sum_{n=1}^{\infty} \exp\left(-\frac{\pi^2 n \varepsilon}{\gamma(\Delta q)^2}\right) = \frac{2}{\Delta q} \sum_{n=1}^{\infty} r^n, \end{aligned}$$

and since $e^z - 1 > z^s/s!$ for all $z > 0$ and all $s \in \mathbb{N}$, we conclude that

$$\sum_{n=1}^{\infty} r^n = r \sum_{n=0}^{\infty} r^n = \frac{r}{1-r} = \frac{1}{\exp(\pi^2\varepsilon/\gamma(\Delta q)^2) - 1} < \frac{s!\gamma^s}{\pi^{2s}\varepsilon^s} (\Delta q)^{2s}.$$

Moreover, a short calculation proves that $S(\Gamma_q; \bullet)$ is Δq -periodic:

$$S(\Gamma_q; x + \Delta q) = \sum_{k \in \mathbb{Z}} g(x - (k-1) \cdot \Delta q)^2 = S(\Gamma_q; x), \quad x \in \mathbb{R}.$$

By the Weierstrass test, see e.g. [WW96, §3.34], the infinite sum converges absolutely and uniformly on any set and therefore, by its periodicity, it follows that $S(\Gamma_q; \bullet) \in C^\infty(\mathbb{R})$. \square

The expansion in (2.3) can also be used in higher dimensions, provided that the position grid $\{q_k\}_{k \in \Gamma_q}$ is aligned to the eigenvectors of the symmetric width matrix $G \in \mathbb{R}^{d \times d}$. The spectral theorem yields that we find an orthogonal matrix $U \in \mathbb{R}^{d \times d}$ and a diagonal matrix $D \in \mathbb{R}^{d \times d}$ such that $G = UDU^T$. In particular, the columns $u_1, \dots, u_d \in \mathbb{R}^d$ of U are given by the eigenvectors of G , building an orthonormal basis of \mathbb{R}^d , whereas the entries of D are given by the corresponding eigenvalues $\lambda_1, \dots, \lambda_d > 0$. If there exist index sets $\Gamma_q^{(1)}, \dots, \Gamma_q^{(d)} \subseteq \mathbb{Z}$, such that

$$\Gamma_q = \Gamma_q^{(1)} \times \dots \times \Gamma_q^{(d)},$$

and for all $k \in \Gamma_q$ we find $\Delta q_1, \dots, \Delta q_d > 0$ such that

$$q_k = \sum_{j=1}^d k_j \Delta q_j u_j,$$

then, the summation curve can be decomposed for all $x \in \mathbb{R}^d$ as

$$S(\Gamma_q; x) = \prod_{j=1}^d \left(\sum_{k_j \in \Gamma_q^{(j)}} g_{k_j}^{(j)}(y_j)^2 \right),$$

where we introduced the variable $y := U^T x$ and, for all $k_j \in \Gamma_q^{(j)}$, the one-dimensional shifted Gaussian functions $g_{k_j}^{(j)}$ are given by

$$g_{k_j}^{(j)}(y) = (\pi\varepsilon)^{-1/4} \lambda_j^{1/4} \exp\left(-\frac{\lambda_j}{2\varepsilon} (y - k_j \Delta q_j)^2\right), \quad y \in \mathbb{R}.$$

A.1. Estimates for the Summation Curve. For the proof of Lemma 3.1 we use two bounds: The first one is an upper bound for the infinite series

$$\sum_{k \in \mathbb{Z}} g(x - q_k),$$

and the second one is a lower bound for the summation curve $S(\Gamma_q; \bullet)$, defined on the finite uniform grid in (3.2).

Lemma A.1. *Let $\{q_k\}_{k \in \mathbb{Z}}$ be a uniform infinite grid of size $\Delta q > 0$ and g the Gaussian amplitude in (2.1) of width $\gamma > 0$. Then, for all $x \in \mathbb{R}$, we have*

$$(A.2) \quad \sum_{k \in \mathbb{Z}} g(x - q_k) < c_{\Delta q, \varepsilon, \gamma},$$

with upper bound $c_{\Delta q, \varepsilon, \gamma} = \sqrt{2}(\pi\varepsilon)^{1/4}\gamma^{-1/4}\frac{1}{\Delta q} (1 + \Delta q\sqrt{\frac{\gamma}{2\pi\varepsilon}})$.

Proof. Using the formula (A.1), we get for all $x \in \mathbb{R}$:

$$\sum_{k \in \mathbb{Z}} g_k(x) \leq \sqrt{2}(\pi\varepsilon)^{1/4}\gamma^{-1/4}\frac{1}{\Delta q} \left(1 + 2 \sum_{n=1}^{\infty} \exp\left(-\frac{2\varepsilon\pi^2 n^2}{\gamma\Delta q^2}\right) \right).$$

Hence, (A.2) follows by the estimate

$$\sum_{n=1}^{\infty} \exp\left(-\frac{2\varepsilon\pi^2 n^2}{\gamma\Delta q^2}\right) \leq \int_0^{\infty} \exp\left(-\frac{2\varepsilon\pi^2 z^2}{\gamma\Delta q^2}\right) dz = \frac{\Delta q}{2} \sqrt{\frac{\gamma}{2\pi\varepsilon}}.$$

□

Lemma A.2. *There exists a positive constant $C_{\Gamma_q, \varepsilon, \gamma} > 0$, depending on ε, γ and the choice of the grid $\{q_k\}_{k \in \Gamma_q}$, such that for all $x \in [q_0 - L_q, q_0 + L_q]$ we have*

$$(A.3) \quad S(\Gamma_q; x) > C_{\Gamma_q, \varepsilon, \gamma}.$$

Proof. We start with the finite uniform grid. Let $\bar{x} \in \Lambda_x$ and denote by q_K the nearest grid point. Hence, there exists $t \in (-\Delta q/2, \Delta q/2]$ such that $\bar{x} = q_K + t$, and without any loss of generality we assume that $t \geq 0$. Now, we decompose the summation curve as

$$S(\Gamma_q; x) = S_K(x) + (S(\Gamma_q; x) - S_K(x)),$$

where the sum S_K is defined for all $x \in \mathbb{R}$ by

$$S_K(x) := \sum_{k=1}^K g(x - q_k)^2.$$

In particular, S_K is symmetric to the axis

$$x = \begin{cases} q_l, & \text{if } K = 2l - 1, \\ q_l + \Delta q/2, & \text{if } K = 2l. \end{cases}$$

Since S_K is strictly increasing on $[q_0 - L_q, q_1]$ and $S(\Gamma_q; \bullet) - S_K$ is strictly increasing on $[q_0 - L_q, q_{K+1}]$, we conclude that

$$S(\Gamma_q; q_0 - L_q) < S_K(q_1 - t) + (S(\Gamma_q; \bar{x}) - S_K(\bar{x})) = S(\Gamma_q; \bar{x}),$$

which shows that on Λ_x the summation curve attains its minimum at $q_0 - L_q$. Using that the Gaussian amplitude function g is monotone decreasing on $[0, \infty)$, we obtain

$$S(\Gamma_q; q_0 - L_q) > \frac{1}{2\Delta q} \frac{2}{\sqrt{\pi}} \int_{\Delta q\sqrt{\gamma/\varepsilon}}^{M\Delta q\sqrt{\gamma/\varepsilon}} e^{-z^2} dz.$$

Hence, (A.3) follows for

$$(A.4) \quad C_{\Gamma_q, \varepsilon, \gamma} = \frac{1}{2\Delta q} \left(\operatorname{erf}\left(2L_q\sqrt{\frac{\gamma}{\varepsilon}}\right) - \operatorname{erf}\left(\Delta q\sqrt{\frac{\gamma}{\varepsilon}}\right) \right).$$

For the uniform infinite grid, the summation curve is Δq -periodic. Hence it is enough to look for its minimum on the interval $[0, \Delta q)$. We estimate for $x \in [0, \Delta q)$ and $k \in \mathbb{Z}$ that

$$|x - k\Delta q| \leq (|k| + 1)\Delta q$$

and therefore

$$g(x - q_k)^2 \geq (\pi\varepsilon)^{-1/2}\gamma^{1/2} \exp\left(-\frac{\gamma}{\varepsilon}((|k| + 1)\Delta q)^2\right).$$

Consequently,

$$S(\Gamma_q; x) \geq (\pi\varepsilon)^{-1/2}\gamma^{1/2} 2 \sum_{k \geq 2} \exp\left(-\frac{\gamma}{\varepsilon}(k\Delta q)^2\right).$$

We estimate

$$\begin{aligned} \sum_{k \geq 2} \exp\left(-\frac{\gamma}{\varepsilon}(k\Delta q)^2\right) &\geq \int_2^\infty \exp\left(-\frac{\gamma}{\varepsilon}(x\Delta q)^2\right) dx \\ &= \sqrt{\frac{\varepsilon}{\gamma}} \frac{1}{\Delta q} \int_{\sqrt{\frac{\varepsilon}{\gamma}} 2\Delta q}^\infty \exp(-z^2) dz = \sqrt{\frac{\varepsilon}{\gamma}} \frac{\sqrt{\pi}}{2\Delta q} \operatorname{erfc}(\sqrt{\gamma/\varepsilon} \cdot 2\Delta q) \end{aligned}$$

and therefore (A.3) follows for

$$(A.5) \quad C_{\Gamma_q, \varepsilon, \gamma} = \frac{1}{\Delta q} \operatorname{erfc}\left(2\Delta q \sqrt{\frac{\gamma}{\varepsilon}}\right).$$

□

Recall that according to Lemma 2.1 the summation curve approximates the constant value $1/\Delta q$ for the infinite uniform grid of size Δq . We notice that this result is in accordance with the bound in (A.3) for the constant $C_{\Gamma_q, \varepsilon, \gamma}$ in (A.5), where $1/\Delta q$ appears as a factor and

$$\operatorname{erfc}\left(2\Delta q \sqrt{\frac{\gamma}{\varepsilon}}\right) \rightarrow 1 \quad \text{as } \Delta q \rightarrow 0.$$

In addition, for the finite uniform grid we recognize the prefactor $1/2\Delta q$ in (A.4), which reflects the fact that at the boundaries of the finite interval Λ_x we are only considering one side of an infinite summation curve and thus have to divided by 2.

Proof (of Lemma 3.1). By the upper bound in (A.2) and the lower bound in (A.3), we conclude that, for all $x \in \Lambda_x$,

$$\frac{1}{S(\Gamma_q; x)} \sum_{k \in \Gamma_q} g(x - q_k) < \frac{C_{\Delta q, \varepsilon, \gamma}}{C_{\Gamma_q, \varepsilon, \gamma}}.$$

In particular, for $\Gamma_q = \{1, \dots, M\}$ the bound in Lemma 3.1 follows for

$$C_{\Gamma_q} = \frac{2\sqrt{2}(\pi\varepsilon)^{1/4}\gamma^{-1/4} (1 + \Delta q \sqrt{\frac{\gamma}{2\pi\varepsilon}})}{(\operatorname{erf}(2L_q \sqrt{\frac{\gamma}{\varepsilon}}) - \operatorname{erf}(\Delta q \sqrt{\frac{\gamma}{\varepsilon}}))},$$

which is bounded in M and

$$\lim_{M \rightarrow \infty} C_{\Gamma_q} = \frac{2\sqrt{2}(\pi\varepsilon)^{1/4}\gamma^{-1/4}}{\operatorname{erf}(2L_q \sqrt{\frac{\gamma}{\varepsilon}})},$$

where we used that $\Delta q \rightarrow 0$ as $M \rightarrow \infty$ and $\operatorname{erf}(x) \rightarrow 0$ as $x \rightarrow 0$. □

APPENDIX B. REPRESENTATION FOR NON-GAUSSIANS

Qian and Ying present a wave packet transform, which is based on compactly supported basis functions that approximate a Gaussian profile, see [QY10, §3]. For instance, in the one-dimensional setup we can think of our basis functions $g_{j,k}$

multiplied by a compactly supported window $w_{\rho,\lambda}$, where the window parameters $0 \leq \rho < \lambda$ are chosen such that the following conditions are fulfilled:

- (1) $0 \leq w_{\rho,\lambda}(x) \leq 1$, for $x \in (-\lambda, \lambda)$;
- (2) $w_{\rho,\lambda}(x) = 0$, for $x \in \mathbb{R} \setminus (-\lambda, \lambda)$;
- (3) $w_{\rho,\lambda}(x) = 1$, for $x \in [-\rho, \rho]$;

If we use the uniformly distributed grid points $q_k = k\lambda$, $p_j = j\pi\varepsilon/\lambda$ and denote by

$$g^w := g \cdot w_{\rho,\lambda}(\bullet - q_k) \quad \text{and} \quad S^w := \sum_{k \in \mathbb{Z}} g^w(\bullet - q_k)^2$$

the windowed Gaussian amplitude and the windowed summation curve, respectively, it can be shown, see [QY10, Lemma 3.1], that the families

$$(B.1) \quad \left\{ \frac{1}{\sqrt{2\lambda}} g_{j,k}^w \right\}_{j,k \in \mathbb{Z}} \quad \text{and} \quad \left\{ \frac{1}{\sqrt{2\lambda}} \frac{1}{S^w} g_{j,k}^w \right\}_{j,k \in \mathbb{Z}}$$

form two frames of $L^2(\mathbb{R})$ (or more general of $L^2(\mathbb{R}^d)$, for an appropriate definition of multidimensional compactly supported basis functions). Frames can be used to recover elements of a Hilbert space with a family of not necessarily linear independent vectors. The theory was developed by Duffin and Schaeffer in [DS52] and they are used nowadays in different directions like signal processing, see e.g. [Mal09, chapter 5]. In particular, frames have been generalized to the continuous setting, which allows an alternative description of several function spaces, see e.g. [FR05]. A reconstruction of an arbitrary function $\psi \in L^2(\mathbb{R}^d)$ can be performed by using the dual frame, see [Mal09, chapter 5.1.2]. In particular, Qian and Ying prove that the frames in (B.1) form dual frames, see [QY10, Lemma 3.2]. Using the notation of this paper here, they get a multivariate analog of the following representation:

Proposition B.1. *For any $\psi \in L^2(\mathbb{R})$ we have*

$$(B.2) \quad \psi = \sum_{k \in \mathbb{Z}} \sum_{j \in \mathbb{Z}} \left\langle \frac{1}{\sqrt{2\lambda}} g_{j,k}^w, \psi \right\rangle \frac{1}{\sqrt{2\lambda}} \frac{1}{S^w} g_{j,k}^w = \frac{1}{S^w} \sum_{k \in \mathbb{Z}} \sum_{j \in \mathbb{Z}} r_{j,k}^w g_{j,k}^w,$$

where the complex-valued representation coefficients $r_{j,k}^w \in \mathbb{C}$ are given by

$$r_{j,k}^w = \frac{\Delta p}{2\pi\varepsilon} \langle g_{j,k}^w, \psi \rangle.$$

The proof of the identity in (B.2) crucially uses that $r_{j,k}^w$ can be viewed as the j th Fourier coefficient of the windowed function $\psi g^w(\bullet - q_k)$. In addition to the proof of Qian and Ying, we present a new proof of (B.2), that is based on windowed Fourier series and allows to calculate the decay of representation coefficients $r_{j,k}$.

Proof (of Proposition B.1 via windowed Fourier series).

Let $\psi \in L^2(\mathbb{R})$. Moreover, for $0 \leq \rho < \lambda$ let $w_{\rho,\lambda} \in C_c^\infty(\mathbb{R})$ be a bump window, satisfying the three conditions above. For $k \in \mathbb{Z}$ we introduce the windowed function

$$\psi_k^w := \psi g^w(\bullet - q_k) \in L^2(\mathbb{R}).$$

In particular, ψ_k^w is compactly supported in $[q_k - \lambda, q_k + \lambda]$. We represent ψ_k^w almost everywhere in $[q_k - \lambda, q_k + \lambda]$ via its windowed Fourier series, see [BL20, Corollary 4.5], as

$$\psi_k^w(x) = \sum_{j \in \mathbb{Z}} c_k^w(j) e^{\frac{i}{\varepsilon} p_j x},$$

where the grid points p_j are given by $p_j = j\pi\varepsilon/\lambda$ and the windowed Fourier coefficients c_k^w are given for all $j \in \mathbb{Z}$ by

$$c_k^w(j) = \frac{1}{2\lambda} \int_{q_k-\lambda}^{q_k+\lambda} \psi_k^w(x) e^{-\frac{i}{\varepsilon} p_j x} dx = \frac{1}{2\lambda} \int_{\mathbb{R}} \psi(x) g^w(x - q_k) e^{-\frac{i}{\varepsilon} p_j x} dx.$$

In particular, for all $j, k \in \mathbb{Z}$ we conclude that

$$c_k^w(j) e^{\frac{i}{\varepsilon} p_j q_k} = \frac{1}{2\lambda} \int_{\mathbb{R}} \psi(x) \overline{g_{j,k}^w(x)} dx = \frac{\Delta p}{2\pi\varepsilon} \langle g_{j,k}^w, \psi \rangle = r_{j,k}^w,$$

which yields that

$$(B.3) \quad c_k^w(j) e^{\frac{i}{\varepsilon} p_j x} = r_{j,k}^w e^{\frac{i}{\varepsilon} p_j (x - q_k)} \quad \text{for all } x \in \mathbb{R}.$$

Consequently, using that $g^w(\bullet - q_k)$ is compactly supported in $[q_k - \lambda, q_k + \lambda]$, we obtain almost everywhere on \mathbb{R} :

$$\begin{aligned} \psi(x) &= \psi(x) \left(\frac{1}{S^w(x)} \sum_{k \in \mathbb{Z}} g^w(x - q_k)^2 \right) = \frac{1}{S^w(x)} \sum_{k \in \mathbb{Z}} \psi_k^w(x) g^w(x - q_k) \\ &= \frac{1}{S^w(x)} \sum_{k \in \mathbb{Z}} \left(\sum_{j \in \mathbb{Z}} c_k^w(j) e^{\frac{i}{\varepsilon} p_j x} \right) g^w(x - q_k) = \sum_{k \in \mathbb{Z}} \sum_{j \in \mathbb{Z}} r_{j,k}^w g_{j,k}^w(x). \end{aligned}$$

□

We note that in order to guarantee that the summation curve is strictly positive, we have to assume that consecutive basis functions $g^w(\bullet - q_k)$ and $g^w(\bullet - q_{k+1})$ are overlapping. For example, this is ensured by the choice $\rho < \Delta q/2$.

Since it follows by (B.3) that

$$|r_{j,k}^w| = |c_k^w(j)| \quad \text{for all } j, k \in \mathbb{Z},$$

the decay rate of $r_{j,k}^w$ with respect to j is given by the decay of the windowed Fourier coefficients of the compactly supported function ψ_k^w . It is known that the compact support limits the decay rate to be at most root exponential and the actual rate depends on the smoothness of the function. For a detailed discussion on windowed Fourier coefficients we refer to [Tad07] and [BL20]. On the other hand side, for the decay rate of $|r_{j,k}^w|$ with respect to k , we can prove spectral convergence if ψ is a Schwartz function:

Lemma B.2. *Let $\psi \in \mathcal{S}(\mathbb{R})$ and assume that the window $w_{\rho,\lambda}$ is even, that is, $w_{\rho,\lambda}(-x) = w_{\rho,\lambda}(x)$ for all $x \in \mathbb{R}$. For all $s \geq 1$, there exists a positive constant $C_s > 0$, depending on $s, \psi, w_{\rho,\lambda}, \lambda, \varepsilon$ and γ , such that, uniformly in $j \in \mathbb{Z}$,*

$$|r_{j,k}^w| \leq \frac{C_s}{|k|^{s+1}} \quad \text{for all } k \neq 0.$$

Proof. The relation in (B.3) yields for all $j, k \in \mathbb{Z}$:

$$|r_{j,k}^w| \leq \frac{1}{2\lambda} \int_{\mathbb{R}} |\psi(x) g^w(x - q_k)| dx.$$

Therefore, using that the window is an even function, we conclude that

$$|r_{j,k}^w| \leq \frac{\|g\|_{\infty}}{2\lambda} \int_{\mathbb{R}} |\psi(x) w_{\rho,\lambda}(q_k - x)| dx = \frac{(\pi\varepsilon)^{-1/4} \gamma^{1/4}}{2\lambda} (|\psi| * w_{\rho,\lambda})(q_k).$$

By [Fol99, Proposition 8.11] it follows that $|\psi| * w_{\rho,\lambda}$ is a real and non-negative Schwartz function. Consequently, there exists a positive constant $c(s, \psi, w_{\rho,\lambda}) > 0$ such that, for all $s \geq 1$ and all $x \in \mathbb{R} \setminus \{0\}$, we have

$$(|\psi| * w_{\rho,\lambda})(x) \leq \frac{c(s, \psi, w_{\rho,\lambda})}{|x|^{s+1}}.$$

Hence, the claim follows for the constant

$$C_s = c(s, \psi, w_{\rho,\lambda}) \frac{(\pi\varepsilon)^{-1/4} \gamma^{1/4}}{2\lambda^{s+2}},$$

where we used that $q_k = k\lambda$. □

REFERENCES

- [BD93] Günter Baszenki and Franz-Jürgen Delyos. *Multivariate Boolean Midpoint Rules*, pages 1–11. Birkhäuser Basel, Basel, 1993.
- [BL20] Paul Bergold and Caroline Lasser. Fourier series windowed by a bump function. *Journal of Fourier Analysis and Applications*, 26(4):65, 2020.
- [BNM00] M Ben-Nun and Todd J Martinez. Photodynamics of ethylene: ab initio studies of conical intersections. *Chemical Physics*, 259(2):237 – 248, 2000.
- [CDS03] M. Chiani, D. Dardari, and M. K. Simon. New exponential bounds and approximations for the computation of error probability in fading channels. *IEEE Transactions on Wireless Communications*, 2(4):840–845, July 2003.
- [CR12] Monique Combescure and Didier Robert. *Coherent states and applications in mathematical physics*. Theoretical and Mathematical Physics. Springer, Dordrecht, 2012.
- [DLCS00] G. Dattoli, S. Lorenzutta, C. Cesarano, and D. Sacchetti. Higher order derivatives of exponential functions and generalized forms of Kampé de Fériet-Bell polynomials. *Int. J. Math. Stat. Sci.*, 9(2):111–123, 2000.
- [DR07] Philip J. Davis and Philip Rabinowitz. *Methods of numerical integration*. Dover Publications, Inc., Mineola, NY, 2007. Corrected reprint of the second (1984) edition.
- [DS52] R. J. Duffin and A. C. Schaeffer. A class of nonharmonic Fourier series. *Trans. Amer. Math. Soc.*, 72:341–366, 1952.
- [Fol89] Gerald B. Folland. *Harmonic analysis in phase space*, volume 122 of *Annals of Mathematics Studies*. Princeton University Press, Princeton, NJ, 1989.
- [Fol99] Gerald B. Folland. *Real analysis*. Pure and Applied Mathematics (New York). John Wiley & Sons, Inc., New York, second edition, 1999. Modern techniques and their applications, A Wiley-Interscience Publication.
- [FR05] Massimo Fornasier and Holger Rauhut. Continuous frames, function spaces, and the discretization problem. *J. Fourier Anal. Appl.*, 11(3):245–287, 2005.
- [FS98] Hans G. Feichtinger and Thomas Strohmer. *Gabor analysis and algorithms*. Applied and Numerical Harmonic Analysis. Birkhäuser Boston, Inc., Boston, MA, 1998. Theory and applications.
- [Gab46] D. Gabor. Theory of communication. Part 1: The analysis of information. *Journal of the Institution of Electrical Engineers - Part III: Radio and Communication Engineering*, 93(26):429–441, November 1946.
- [GG98] Thomas Gerstner and Michael Griebel. Numerical integration using sparse grids. *Numer. Algorithms*, 18(3-4):209–232, 1998.
- [Grö01] Karlheinz Gröchenig. *Foundations of time-frequency analysis*. Applied and Numerical Harmonic Analysis. Birkhäuser Boston, Inc., Boston, MA, 2001.
- [GS00] Michael Griebel and Marc Alexander Schweitzer. A particle-partition of unity method for the solution of elliptic, parabolic, and hyperbolic PDEs. *SIAM J. Sci. Comput.*, 22(3):853–890, 2000.
- [KMB16] Xiangmeng Kong, Andreas Markmann, and Victor S. Batista. Time-sliced thawed gaussian propagation method for simulations of quantum dynamics. *The Journal of Physical Chemistry A*, 120(19):3260–3269, 05 2016.
- [KU98] Arnold R. Krommer and Christoph W. Ueberhuber. *Computational integration*. Society for Industrial and Applied Mathematics (SIAM), Philadelphia, PA, 1998.
- [LF03] E. Larsson and B. Fornberg. A numerical study of some radial basis function based solution methods for elliptic pdes. *Computers and Mathematics with Applications*, 46(5):891 – 902, 2003.
- [LL20] Caroline Lasser and Christian Lubich. Computing quantum dynamics in the semiclassical regime. *Preprint on arXiv*, 2020.

- [LQ09] Shingyu Leung and Jianliang Qian. Eulerian Gaussian beams for Schrödinger equations in the semi-classical regime. *J. Comput. Phys.*, 228(8):2951–2977, 2009.
- [Mal09] Stéphane Mallat. *A wavelet tour of signal processing*. Elsevier/Academic Press, Amsterdam, third edition, 2009. The sparse way, With contributions from Gabriel Peyré.
- [Mar02] André Martinez. *An introduction to semiclassical and microlocal analysis*. Universitext. Springer-Verlag, New York, 2002.
- [MBNL96] Todd J. Martinez, M. Ben-Nun, and R. D. Levine. Multi-electronic-state molecular dynamics: A wave function approach with applications. *The Journal of Physical Chemistry*, 100(19):7884–7895, 1996.
- [ML01] Gary F Margrave and Michael P Lamoureux. Gabor deconvolution. *CREWES Research Report*, 13:241–276, 2001.
- [MM94] G. Mastroianni and G. Monegato. Error estimates for Gauss-Laguerre and Gauss-Hermite quadrature formulas. In *Approximation and computation (West Lafayette, IN, 1993)*, volume 119 of *Internat. Ser. Numer. Math.*, pages 421–434. Birkhäuser Boston, Boston, MA, 1994.
- [MMC90] H.-D. Meyer, U. Manthe, and L.S. Cederbaum. The multi-configurational time-dependent hartree approach. *Chemical Physics Letters*, 165(1):73 – 78, 1990.
- [Nie92] Harald Niederreiter. *Random number generation and quasi-Monte Carlo methods*, volume 63 of *CBMS-NSF Regional Conference Series in Applied Mathematics*. Society for Industrial and Applied Mathematics (SIAM), Philadelphia, PA, 1992.
- [PP02] Athanasios Papoulis and S. Unnikrishna Pillai. *Probability, Random Variables, and Stochastic Processes*. McGraw Hill, Boston, fourth edition, 2002.
- [QY10] Jianliang Qian and Lexing Ying. Fast Gaussian wavepacket transforms and Gaussian beams for the Schrödinger equation. *J. Comput. Phys.*, 229(20):7848–7873, 2010.
- [SI88] Avram Sidi and Moshe Israeli. Quadrature methods for periodic singular and weakly singular fredholm integral equations. *Journal of Scientific Computing*, 3(2):201–231, 1988.
- [Sie43] Carl Ludwig Siegel. Symplectic geometry. *Amer. J. Math.*, 65:1–86, 1943.
- [Tad07] Eitan Tadmor. Filters, mollifiers and the computation of the Gibbs phenomenon. *Acta Numer.*, 16:305–378, 2007.
- [TSM85] D. M. Titterton, A. F. M. Smith, and U. E. Makov. *Statistical analysis of finite mixture distributions*. Wiley Series in Probability and Mathematical Statistics: Applied Probability and Statistics. John Wiley & Sons, Ltd., Chichester, 1985.
- [Tu11] Loring W. Tu. *An introduction to manifolds*. Universitext. Springer, New York, second edition, 2011.
- [WRB04] G. A. Worth, M. A. Robb, and I. Burghardt. A novel algorithm for non-adiabatic direct dynamics using variational gaussian wavepackets. *Faraday Discuss.*, 127:307–323, 2004.
- [WW96] E. T. Whittaker and G. N. Watson. *A course of modern analysis*. Cambridge Mathematical Library. Cambridge University Press, Cambridge, 1996. An introduction to the general theory of infinite processes and of analytic functions; with an account of the principal transcendental functions, Reprint of the fourth (1927) edition.
- [Zhe14] Chunxiong Zheng. Optimal error estimates for first-order Gaussian beam approximations to the Schrödinger equation. *SIAM J. Numer. Anal.*, 52(6):2905–2930, 2014.

(PAUL BERGOLD) ZENTRUM MATHEMATIK, TECHNISCHE UNIVERSITÄT MÜNCHEN, GERMANY
Email address: `bergold@ma.tum.de`

(CAROLINE LASSER) ZENTRUM MATHEMATIK, TECHNISCHE UNIVERSITÄT MÜNCHEN, GERMANY
Email address: `classer@ma.tum.de`